RESEARCH

UDOT

Keeping Utah Moving

Utah Department of Transportation - Research Division
4501 South 2700 West - P.O. Box 148410 - SLC,UT 84114-8410

Report No. UT-21.24

BALANCED ASPHALT CONCRETE MIX PERFORMANCE IN UTAH

PHASE V: FIELD EVALUATION FOR INTERMEDIATE AND LOW-TEMPERATURE CRACKING

Prepared For:

Utah Department of Transportation
Research & Innovation Division

Final Report
July 2021

DISCLAIMER

The authors alone are responsible for the preparation and accuracy of the information, data, analysis, discussions, recommendations, and conclusions presented herein. The contents do not necessarily reflect the views, opinions, endorsements, or policies of the Utah Department of Transportation or the U.S. Department of Transportation. The Utah Department of Transportation makes no representation or warranty of any kind, and assumes no liability therefore.

ACKNOWLEDGMENTS

The authors acknowledge the Utah Department of Transportation (UDOT) for funding this research and the following individuals from UDOT on the Technical Advisory Committee for helping to guide the research:

- Scott Nussbaum
- Howard Anderson
- David Stevens
- Vincent Liu

The authors also acknowledge the following individuals and their work. Most of the information contained in this report is the result of their hard work. This includes the following:

- Abu Sufian Mohammad Asib, Ph.D. University of Utah
- Rizwanur Rahman, Ph.D. candidate, Chemical Engineering, University of Utah
- Abdullahal Mamun, Ph.D. candidate, Civil Engineering, University of Utah
- Tim Biel, PEPG
- Kevin VanFrank, PEPG
- Faramarz Safazadeh, Ph.D., PEPG
- Michael VanMilligen, PEPG
- Clark Allen, Utah Department of Transportation
- Mike White, Utah Department of Transportation

The authors also acknowledge the financial contribution from the Mountain-Plains Consortium.

TECHNICAL REPORT ABSTRACT

1. Report No. UT-21.24	2. Government Accession No. N/A	3. Recipient's Catalog No. N/A
4. Title and Subtitle BALANCED ASPHALT CONCRETE MIX PERFORMANCE IN UTAH. PHASE V: FIELD EVALUATION FOR INTERMEDIATE AND LOW-TEMPERATURE CRACKING		5. Report Date July 2021 6. Performing Organization Code N/A
7. Author(s) Pedro Romero, Ph.D., P.E.		8. Performing Organization Report No. N/A
9. Performing Organization Name and Address University of Utah Department of Civil and Environmental Engineering 110 Central Campus Drive, Suite 2000 Salt Lake City, UT, 84112		10. Work Unit No. 5H08423H 11. Contract or Grant No. 20-8639
12. Sponsoring Agency Name and Address Utah Department of Transportation 4501 South 2700 West P.O. Box 148410 Salt Lake City, UT 84114-8410		13. Type of Report & Period Covered Final Dec. 2019 – July 2021 14. Sponsoring Agency Code PIC No. UT19.105
15. Supplementary Notes Prepared in cooperation with the Utah Department of Transportation and the U.S. Department of Transportation, Federal Highway Administration		

16. Abstract

A follow-up study was conducted in which the performance of five asphalt pavements was documented after three years of field service in Utah. Cores were taken at each pavement section and brought to the lab where they were cut and tested using the BBR, the IFIT, and the IDEAL CT. The respective performance indices from these tests were compared to the previous results obtained from the loose mix obtained at the time of construction.

The predicted performance from the original study was compared to the actual performance of the pavement sections. Based on the test results from laydown material, it was found that the BBR was correct in predicting poor low-temperature performance and the IFIT was also able to predict poor intermediate temperature performance. These results can help in setting a threshold that new mixtures must meet for good performance. For the BBR, a maximum creep modulus of 12,000 MPa and a minimum m-value of 0.12, at the expected environmental conditions, were found. Furthermore, the effect of aging should be considered. For the FI a minimum value of 8 at 25 ºC was found, and, based on a relation between the FI and the CT Index, a minimum CT Index of 125 to 150 was estimated. Finally, the chemical changes of standard asphalt mixtures from aging and the introduction of RAP were studied using FT-IR and SEM. The results showed an inverse relation between the formation of certain chemical groups produced from the oxidation of the material and the mechanical properties.

The final conclusion of this study was that mechanical tests such as the BBR at low temperatures and the IDEAL CT at intermediate temperatures performed on recently produced asphalt mixtures can predict those sections that are likely to show poor performance. It is recommended that such tests be adopted as part of the asphalt mixture design process within UDOT.

17. Key Words Asphalt mixtures, performance testing, bending beam rheometer, flexibility index, IDEAL CT, oxidation, SEM.		18. Distribution Statement Not restricted. Available through: UDOT Research & Innovation Div. 4501 South 2700 West P.O. Box 148410 Salt Lake City, UT 84114-8410 www.udot.utah.gov/go/research		23. Registrant's Seal N/A
19. Security Classification (of this report) Unclassified	20. Security Classification (of this page) Unclassified	21. No. of Pages 60	22. Price N/A	

TABLE OF CONTENTS

LIST OF TABLES

LIST OF FIGURES

UNIT CONVERSION FACTORS

Units used in this report and not conforming to the UDOT standard unit of measurement (U.S. Customary system) are given below with their U.S. Customary equivalents:

SI* (MODERN METRIC) CONVERSION FACTORS

APPROXIMATE CONVERSIONS TO SI UNITS

Symbol	When You Know	Multiply By	To Find	Symbol
		LENGTH		
in	inches	25.4	millimeters	mm
ft	feet	0.305	meters	m
yd	yards	0.914	meters	m
mi	miles	1.61	kilometers	km
		AREA		
in^2	square inches	645.2	square millimeters	mm^2
ft^2	square feet	0.093	square meters	m^2
yd^2	square yard	0.836	square meters	m^2
ac	acres	0.405	hectares	ha
mi^2	square miles	2.59	square kilometers	km^2
		VOLUME		
fl oz	fluid ounces	29.57	milliliters	mL
gal	gallons	3.785	liters	L
ft^3	cubic feet	0.028	cubic meters	m^3
yd^3	cubic yards	0.765	cubic meters	m^3
	NOTE: volumes greater than 1000 L shall be shown in m^3			
		MASS		
oz	ounces	28.35	grams	g
lb	pounds	0.454	kilograms	kg
T	short tons (2000 lb)	0.907	megagrams (or "metric ton")	Mg (or "t")
		TEMPERATURE (exact degrees)		
°F	Fahrenheit	5 (F-32)/9 or (F-32)/1.8	Celsius	°C
		ILLUMINATION		
fc	foot-candles	10.76	lux	lx
fl	foot-Lamberts	3.426	$candela/m^2$	cd/m^2
		FORCE and PRESSURE or STRESS		
lbf	poundforce	4.45	newtons	N
lbf/in^2	poundforce per square inch	6.89	kilopascals	kPa

APPROXIMATE CONVERSIONS FROM SI UNITS

Symbol	When You Know	Multiply By	To Find	Symbol
		LENGTH		
mm	millimeters	0.039	inches	in
m	meters	3.28	feet	ft
m	meters	1.09	yards	yd
km	kilometers	0.621	miles	mi
		AREA		
mm^2	square millimeters	0.0016	square inches	in^2
m^2	square meters	10.764	square feet	ft^2
m^2	square meters	1.195	square yards	yd^2
ha	hectares	2.47	acres	ac
km^2	square kilometers	0.386	square miles	mi^2
		VOLUME		
mL	milliliters	0.034	fluid ounces	fl oz
L	liters	0.264	gallons	gal
m^3	cubic meters	35.314	cubic feet	ft^3
m^3	cubic meters	1.307	cubic yards	yd^3
		MASS		
g	grams	0.035	ounces	oz
kg	kilograms	2.202	pounds	lb
Mg (or "t")	megagrams (or "metric ton")	1.103	short tons (2000 lb)	T
		TEMPERATURE (exact degrees)		
°C	Celsius	1.8C+32	Fahrenheit	°F
		ILLUMINATION		
lx	lux	0.0929	foot-candles	fc
cd/m^2	$candela/m^2$	0.2919	foot-Lamberts	fl
		FORCE and PRESSURE or STRESS		
N	newtons	0.225	poundforce	lbf
kPa	kilopascals	0.145	poundforce per square inch	lbf/in^2

*SI is the symbol for the International System of Units. (Adapted from FHWA report template, Revised March 2003)

LIST OF ACRONYMS

AASHTO – American Association of State Highway and Transportation Officials

ASTM – American Society of Testing and Materials

BBR – Bending Beam Rheometer, refers to AASHTO TP-125

BSE – Backscatter Electron

C/O Ratio – Carbon-to-oxygen ratio

CT Index – Cracking Tolerance Index

EDX – Energy Dispersing X-Ray

FI – Flexibility Index, refers to AASHTO TP-124

FT IR – Fourier Transform Infrared Spectroscopy

IDEAL CT - Indirect Tension Asphalt Cracking Tests, refers to ASTM D8225

IFIT – Illinois Flexibility Index Tests, refers to AASHTO TP-124

NMAS – Nominal Maximum Aggregate Size

RAP – Recycled Asphalt Pavement

SCB – Semi-Circular Bending

SEM - Scanning Electron Microscopy

UDOT – Utah Department of Transportation

U of U – University of Utah

UV – Ultra Violet, radiation with shorter wavelength than visible light

EXECUTIVE SUMMARY

A follow-up study was conducted in which the performance of five pavement sections from different asphalt mixtures was documented after three years of field service in Utah. Cores were taken at each pavement section and brought to the University of Utah where they were cut into the appropriate specimen configuration and tested using the BBR (AASHTO TP125), the IFIT (AASHTO TP124), and the IDEAL CT (ASTM 8225). These tests provided the field-age properties of the material at low and intermediate temperatures. The respective performance indices from these tests were compared to the results previously obtained from the loose mix obtained at the time of construction, thus showing the changes caused by aging on the mechanical properties.

The predicted performance based on the BBR and the IFIT from the original study was compared to the actual performance of the pavement sections. Based on the results from laydown material, it was found that the BBR was correct in predicting poor low-temperature performance and the IFIT was also able to predict poor intermediate-temperature performance. These results can help in setting a threshold or target value that new mixtures must meet for good performance expectations. For the BBR, a maximum creep modulus of 12,000 MPa and a minimum m-value of 0.12, at the expected environmental conditions (i.e., low pavement temperature), were found. Mixture degradation in the form of microcracking from the aging process should also be evaluated. For the IFIT, a minimum FI value of 8 at 25 ºC was found, and, based on a relation developed between the FI from the IFIT and the CT Index from the IDEAL CT, a minimum CT Index of 125 to 150 was estimated. However, this relation was developed based on limited data so more testing is required.

Finally, the chemical changes of standard asphalt mixtures from aging and the introduction of RAP were studied using FT-IR. The results showed an inverse relation between the formation of certain chemical groups such as alcohols, acids, and carbonyls that are produced from the oxidation of the material and the mechanical properties at low temperatures. These results were validated using SEM. Analysis of SEM images showed the development of microcracks in the specimens which explain why, in some cases, the creep modulus of mixtures decreases after long-term aging.

The final conclusion of this study was that mechanical tests such as the BBR at low temperatures and the IDEAL CT at intermediate temperatures performed on recently produced asphalt mixtures can predict those sections that are likely to show poor performance. It is recommended that such tests be adopted as part of the asphalt mixture design process within UDOT.

1.0 INTRODUCTION

1.1 Problem Statement

Utah DOT's pavements are its largest and most expensive asset. Within its current practice, UDOT is using aggressive rutting and stripping testing to qualify asphalt mixes for use in highway construction. This practice was in response to the typical distresses found in pavements from the late 1980s and early 1990s. In Utah, as well as in other states, this has generally resolved rutting issues, but has led to a detrimental effect on cracking and raveling behavior in the pavements. In an attempt to resist rutting, increase recycling efforts, and save costs on materials, mixes now contain Recycled Asphalt Pavement (RAP) and less asphalt binder, both virgin and total. This one-dimensional approach has been recognized as a challenge to be addressed within the mix design process and the Department has been looking for practical tests to provide a performance balance and increase mix durability (i.e., virgin binder content).

The SCB IFIT (AASHTO TP124) and the IDEAL CT (ASTM D8225) have been recognized by UDOT as appropriate tests to measure the intermediate-temperature performance of asphalt mixtures at intermediate temperatures. Current research indicates that the parameters obtained from these tests can identify trends in mixtures that might show poor performance, in terms of fatigue cracking, once placed in the field. A study was conducted where hot-mix asphalt samples were collected from seven different sites, both at the plant and at laydown. The samples were tested using the IFIT resulting in Flexibility Index, FI, values from a low of 3 to a high of 20. While it is known that asphalt mixtures with low FI values will have high propensity for cracking, an actual threshold value has not been determined in the state of Utah. Values between 5 and 10 have been suggested for other states, but it is not known if such values even apply to the asphalt mixtures used in the state of Utah. Anecdotal evaluation of paving mixes placed in Utah over the last 15 years indicates that mixes with a high propensity for cracking typically show early-age cracking as early as year 2 or 3. Based on this information, an evaluation of the field performance of the seven mixtures collected in 2017 was conducted to allow the determination of appropriate thresholds for the FI or an equivalent CT Index for the conditions in Utah.

1.2 Objectives

The objectives of this research are:

1. Evaluate mechanical properties of cores obtained from mixtures previously evaluated during mixing and laydown and relate the mechanical properties to pavement performance observations.
2. Determine if a cracking index such as the FI or CT Index relates to field performance in terms of pavement cracking at intermediate temperatures.
3. Develop a threshold or limiting value for a cracking index for both low-temperature cracking and intermediate-temperature cracking based on the observed pavement condition and considering the aging of the material. Recommend such value to UDOT.
4. Relate FI values to CT-Index values, thus allowing for a transition from IFIT to IDEAL CT testing of mixtures at intermediate temperatures.

1.3 Scope

The scope of this project consists of visual inspections followed by coring and testing of the cores from pavement sections that were placed using asphalt mixtures evaluated on a 2017 study. Complete details of that study can be found in the following UDOT Report:

Balanced Asphalt Concrete Mix Performance in Utah, Phase III: Evaluation of Field Materials Using BBR and SCB-iFIT Tests (UDOT Report No. UT-19.15) by Romero and VanFrank

(See the REFERENCES section for links to referenced reports.)

Pavement evaluation and coring were done by PEPG while testing was done by the University of Utah. Analysis was done as a collaborative process between the University of Utah, PEPG Consulting, and the Utah Department of Transportation.

1.4 Outline of Report

This report contains the following chapters:

- INTRODUCTION
  - provides the background, objectives, and scope of this study
- MATERIALS
  - describes the composition of the materials used in this research
- RESULTS FROM 2020
  - presents the results from BBR, IFIT and IDEAL CT tests
- DATA ANALYSIS
  - interprets results and relations to previous studies
- PERFORMANCE OBSERVATIONS
  - summarizes field observations
- EFFECT OF AGING
  - presents an analysis of the chemical changes in the mix
- CONCLUSIONS
  - includes the conclusions and limitations of this study
- RECOMMENDATIONS AND IMPLEMENTATION
  - recommends future work

2.0 MATERIALS

2.1 Overview

A study was conducted in 2017 (Romero and VanFrank, UDOT Report No. UT-19.15, 2019) where hot-mix asphalt materials were collected from seven different plants and at two locations: at the plant (minimum aging) and at laydown (short-term aging). The asphalt mixtures were brought to the lab where samples were compacted and tested at 25 ºC using the SCB-IFIT configuration, resulting in Flexibility Index, FI, values. Samples were also compacted and cut into small beams for testing in the Bending Beam Rheometer, BBR, at -12 ºC, -18 ºC, and -24 ºC resulting in creep modulus (stiffness) and m-values at those temperatures analyzed at 60 seconds. At the time of the 2017 study, the IDEAL CT was not fully developed, thus it was not used for testing. Since that time, the IDEAL CT test has been favored by UDOT over the SCB-IFIT configuration for intermediate-temperature testing (VanFrank and Romero, UDOT Report No. UT-20.13, 2020).

Anecdotal evaluation of paving mixes placed in Utah over the last 15 years indicates that mixtures with a high propensity for cracking typically show early-age cracking as early as year 2 or 3. Therefore, it was decided to return to the locations where the mixtures were placed in 2017 to evaluate their performance and obtain cores to perform updated testing. Unfortunately, only 5 out of the original sections were available for coring and testing.

2.2 Material Properties

Table 2-1 (Table 3-1 in the 2019 report) shows the material properties of the mixtures tested. Sections in grey were part of the original report but are not included on this report.

As previously mentioned, asphalt mixtures were collected from seven different facilities and at two locations: at the plant and at the field (laydown). At the plant, material was sampled from the conveyor slat as it came from the mixer thus representing aging during mixing (loss of volatiles). At laydown, the material was collected from the windrow dump representing the condition referred to as short-term aging. For all cases, the material was placed in 5-gallon metal buckets and sealed while still hot. The temperature of the material at sampling was recorded.

The material was then transported to a central location where it was distributed to the three testing labs: PEPG, University of Utah, and UDOT Central Lab.

Table 2-1 Material Properties

Mix ID	Design Method	Aggregate NMAS	RAP Content	Total Binder by Mass	Virgin Binder by Mass/ Vol	Virgin Binder	Intended Climate
UT-01	50-Blow Marshall[1]	12.5 mm	30%	5.4%	3.8%/ 9.0%	PG 64-22	Hot
UT-02	75-Blow Marshall[1]	19 mm	30%	4.9%	3.4%/ 9.6%	PG 58-34	Medium
UT-03	75-NDES Superpave[2]	12.5 mm	25%	5.3%	4.0%/ 9.6%	PG 64-34	Cold
UT-04	75-NDES Superpave[2]	12.5 mm	15%	5.3%	4.6%/ 10.9%	PG 64-34	Medium
UT-05	50-Blow Marshall[1]	12.5 mm	30%	6.3%	4.4%/ 10.1%	PG 58-28	Cold
UT-06	75-NDES Superpave[2]	12.5 mm	25%	4.8%	3.7%/ 11.2%	PG 58-28	Cold
UT-07	75 NDES Superpave[2]	12.5 mm	10%	5.3%	4.9%/ 11.1%	PG 64-28	Medium

1. Based on APWA specifications 2. Based on UDOT 2741 specification

- All information provided by supplier and not verified by research team
- Grey mixtures not part of current study

2.3 2017 Testing Results

During the original 2017 study, mixtures were tested in multiple labs. For the present 2020 follow-up study, the cores were tested at the University of Utah lab and not all sections were available. For consistency, only data from the University of Utah, and only for those sections for which cores were eventually taken, is presented here.

2.3.1 BBR Results

The original BBR results (Tables 4-1 and 4-2 in the 2019 report), as reported by the University of Utah laboratory, are shown in Table 2-2.

Table 2-2 Relevant BBR Results at 60 Seconds

	Testing Temperature, °C	**-24**		**-18**		**-12**	
	Sampling Location	**Plant**	**Field[1]**	**Plant**	**Field**	**Plant**	**Field**
	Number of samples	12	12	12	12	12	12
UT-02	**Modulus (MPa)**	**16,692**	**17,808**	**14,075**	**14,958**	**10,562**	**11,437**
	C of Var (%)	12	21	16	18	11	16
	m-value	**0.087**	**0.106**	**0.118**	**0.118**	**0.158**	**0.152**
	C of Var (%)	10	13	11	10	6	9
UT-03	**Modulus (MPa)**	**14,033**	**15,133**	**9,339**	**9,743**	**6,253**	**6,648**
	C of Var (%)	13	8	15	26	21	25
	m-value	**0.126**	**0.121**	**0.170**	**0.169**	**0.241**	**0.242**
	C of Var (%)	10	11	6	10	9	6
UT-04	**Modulus (MPa)**	**13,308**	**10,715**	**10,228**	**7,855**	**6,264**	**4,189**
	C of Var (%)	10	22	7	18	12	17
	m-value	**0.130**	**0.162**	**0.188**	**0.220**	**0.259**	**0.298**
	C of Var (%)	10	12	4	11	4	11
UT-05	**Modulus (MPa)**	**20,083**	**19,917**	**17,167**	**15,408**	**12,408**	**11,921**
	C of Var (%)	11	7	19	13	9	13
	m-value	**0.100**	**0.099**	**0.125**	**0.126**	**0.166**	**0.178**
	C of Var (%)	13	9	11	12	8	6
UT-07	**Modulus (MPa)**	**12,479**	**14,683**	**9,836**	**11,686**	**6,061**	**7,335**
	C of Var (%)	26	13	23	20	19	19
	m-value	**0.138**	**0.122**	**0.189**	**0.167**	**0.248**	**0.243**
	C of Var (%)	12	10	14	8	11	8

[1] Field refers to laydown

2.3.2 2017 Flexibility Index Results

As part of the original study, the FI of each mix was determined at three different laboratories (University of Utah, PEPG/CMT, and UDOT Central Lab), and while the general conclusions and ranking were the same for all labs, the actual FI value varied between labs. The data indicated that one of the labs had higher FI values than the other two labs (see Section 6.2 of the 2019 report). Therefore, to avoid distractions caused by any bias and given that the field cores were only tested at the University of Utah lab, only results from that specific lab are presented in Table 2-3. The complete set of data can be found in Table 6-1 of the 2019 report.

That report also includes an extensive discussion regarding the variability of the test results that is not repeated here.

Table 2-3 Relevant FI Results from U of U Laboratory

		Plant	Field[2]
UT-02	Puck 1	5.5	3.7
	Puck 2	4.3	3.0
	C of Var[1]	29%	24%
	Average[1]	**4.9**	**3.4**
UT-03	Puck 1	12.0	8.7
	Puck 2	4.6	-
	C of Var[1]	20%	27%
	Average[1]	**8.3**	**8.7**
UT-04	Puck 1	15.3	10.0
	Puck 2	8.4	7.4
	C of Var[1]	38%	27%
	Average[1]	**11.8**	**8.7**
UT-05	Puck 1	3.8	4.5
	Puck 2	7.8	9.4
	C of Var[1]	39%	40%
	Average[1]	**5.8**	**7.0**
UT-07	Puck 1	14.3	10.1
	Puck 2	9.0	15.8
	C of Var[1]	28%	29%
	Average[1]	**11.6**	**12.9**

[1] based on 8 samples tested (i.e., both pucks) except for UT-03
[2] field refers to laydown

2.4 Summary

A background of the original study, along with relevant material properties and relevant tests results are given in this chapter. More information can be found in the 2019 report (Romero and VanFrank, UDOT Report No. UT-19.15, 2019).

3.0 RESULTS FROM 2020

3.1 Overview

After three years of the pavement sections being in the field, cores were taken in 5 of the original 7 sections in 2020. The cores were brought to the University of Utah laboratory where they were cut as required and tested using the BBR, the SCB-IFIT, and the IDEAL CT tests. Given that the specimens were obtained from field cores, no air voids were determined.

3.2 Test Results

3.2.1 BBR Results

One core was used to obtain approximately 15 BBR samples. The ten beams that more closely match the required dimension were selected and tested at three temperatures based on the procedures described in AASHTO TP-125. The values at 60 seconds for creep modulus (stiffness) and relaxation capacity (m-value) are shown in Table 3-1. The coefficient of variation (standard deviation divided by the mean) is reported for all 10 data values. As previous research has shown, 10 samples is more than the minimum value required for valid results, and a trimmed mean can be used to ensure greater normality in the data and reduce the coefficient of variation (Asib et.al, 2018; Ho and Martin Linares, 2019). This was not done in this study.

3.2.2 Flexibility Index Results

To determine the flexibility index, FI, two cores were cut to a height of 50 mm, then further cut diametrically and notched, resulting in 4 specimens. Tests were conducted at 25 ºC following the procedures outlined in AASHTO TP-124. Previous research has shown that fracture-type tests might contain outliers resulting in higher than desired variation (VanFrank and Romero, 2020; Safazadeh et al., 2021). It has been recommended that the highest value be eliminated. Table 3-2 shows the results of the FI for all four samples tested as well as for the case where the highest value is eliminated, resulting in an average and standard deviation based on three values.

The results in the table show that testing 4 samples and eliminating the highest value reduces the coefficient of variation from 64% to 28% for UT-02 results and from 48% to 20% for UT-05 results. However, it is noted that the overall results do not change significantly and the relative ranking of the sections remains the same; therefore, the analysis is still presented based on 4 samples.

Table 3-1 BBR Results at 60 Seconds

	Testing Temperature, ºC	**-24**	**-18**	**-12**
	Number of Samples tested	10	10	10
UT-02	**Modulus (MPa)**	**8,410**	**10,034**	**8,007**
	C of Var (%)	36	26	17
	m-value	**0.088**	**0.125**	**0.139**
	C of Var (%)	40	56	28
UT-03	**Modulus (MPa)**	**14,010**	**10,485**	**6,344**
	C of Var (%)	14	9	18
	m-value	**0.137**	**0.171**	**0.226**
	C of Var (%)	9	8	8
UT-04	**Modulus (MPa)**	**16,500**	**11,501**	**7,390**
	C of Var (%)	14	28	18
	m-value	**0.128**	**0.160**	**0.227**
	C of Var (%)	8	18	12
UT-05	**Modulus (MPa)**	**14,341**	**12,889**	**9,256**
	C of Var (%)	39	18	21
	m-value	**0.093**	**0.134**	**0.180**
	C of Var (%)	31	7	9
UT-07	**Modulus (MPa)**	**14,990**	**11,651**	**7,932**
	C of Var (%)	23	16	11
	m-value	**0.116**	**0.155**	**0.204**
	C of Var (%)	14	9	11

3.2.3 CT Index Results

To determine the CT Index, 3 cores were cut to a height of 50-mm and tested at 25 ºC following the procedures outlined in ASTM D8225. The results are shown in Table 3-3. Given the limited number of samples available, even if present, no outliers were eliminated.

Table 3-2 Flexibility Index Results

		FI-4[1]	FI-3[2]
UT-02	**Average**	**1.49**	**1.03**
	C of Var (%)	64	28
UT-03	**Average**	**8.32**	**7.84**
	C of Var (%)	15	12
UT-04	**Average**	**6.63**	**6.22**
	C of Var (%)	17	16
UT-05	**Average**	**3.71**	**2.84**
	C of Var (%)	48	20
UT-07	**Average**	**--**	**3.65**
	C of Var (%)	--	23

[1] based on 4 samples obtained from 2 cores
[2] based on 3 samples after eliminating the highest value

Table 3-3 CT Index Results

		CT Index
UT-02	**Average[1]**	**31.8**
	C of Var (%)[1]	**40**
UT-03	**Average**	**191.8**
	C of Var (%)	**49**
UT-04	**Average**	**66.9**
	C of Var (%)	**11**
UT-05	**Average**	**106.2**
	C of Var (%)	**6**
UT-07	**Average**	**125.0**
	C of Var (%)	**41**

[1] Based on 3 samples each taken from a different core

3.3 Summary

The cores obtained from the five 3-year-old field sections were brought to the University of Utah where they were cut and tested using the BBR, the SCB-IFIT, and the IDEAL CT test configurations. The results are summarized in Tables 3-1, 3-2, and 3-3 for the different tests. Similarly to the previous study, the data shows a wide range of values and differences in performance would be expected. There is also some consistency between tests. Both FI and CT Index show the same sections with low flexibility while the BBR shows it has high modulus and low m-values. In some cases, the variability of the results was higher than desirable.

4.0 DATA ANALYSIS

4.1 Overview

This study was able to obtain data from different mixtures at three different conditions, starting at the plant, then at laydown, and from cores obtained after three years of service. Such unique data allows for an analysis of how the mechanical properties of the material are affected by aging conditions. Looking at the progression of material properties with time will allow setting of a threshold, or limit, that can be used to prevent premature failure. Other relevant information includes the relation between material variability and expected performance as well as the relation between different tests.

4.2 Comparison of Data

The 2017 study results (2019 report) were obtained from laboratory-prepared samples while the 2020 results (current study report) were obtained from field cores. It is known that differences in compaction as well as differences in air voids could affect the results and increase the variability. Furthermore, after being exposed to the environment for several years, the chemical composition of the material has changed due to oxidative aging. Therefore, comparisons between the 2017 and the 2020 data must be done with caution. The effect of aging is further discussed in Chapter 6.0.

4.2.1 Comparison of BBR Data

The results obtained from the BBR at -18 ºC, plotted in a modified Black Space Diagram are shown in Figure 4-1. While not all sections were designed for an environment of -28 ºC (i.e., tests at -18 ºC), looking at one temperature simplifies the analysis. This, however, does not imply that only one temperature is needed to evaluate performance. As it is accepted practice for asphalt binders, the evaluation temperature of mixtures should be based on the intended environment of the material.

Figure 4-1 shows sections UT-02 and UT-05 plotting on the upper left quadrant of the Black Space diagram. Sections that plot on this quadrant have high creep modulus and low

relaxation capacity, both indicators of expected poor low-temperature cracking performance (Jones et al., 2014).

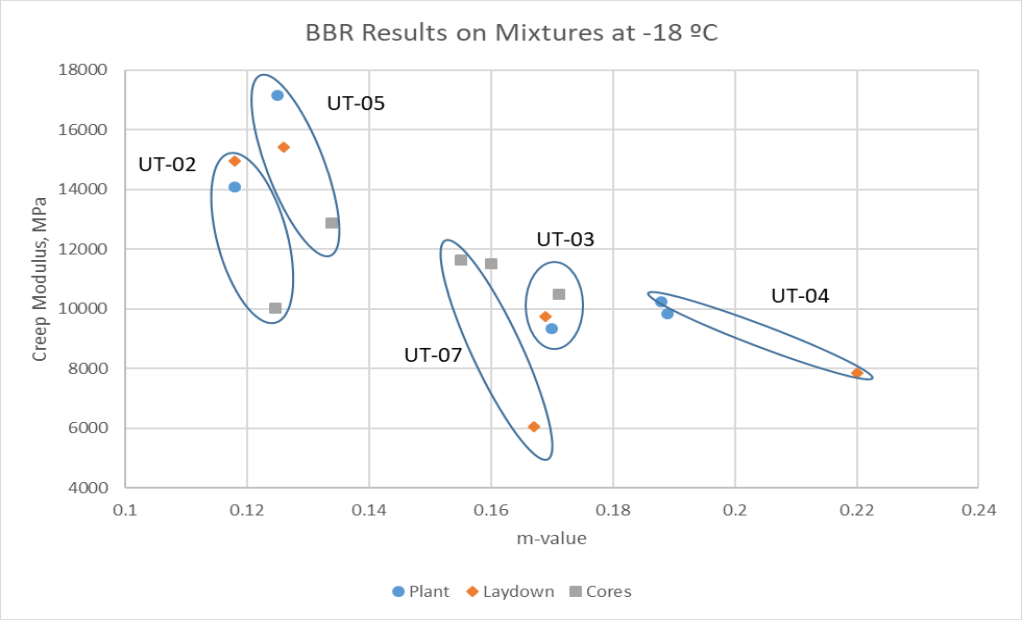

Figure 4-1 Black Space Diagram at -18 ºC

To isolate the changes in material properties caused by aging, the results for the creep modulus only are shown in Figure 4-2; the results for the m-value are shown separately on Figure 4-3.

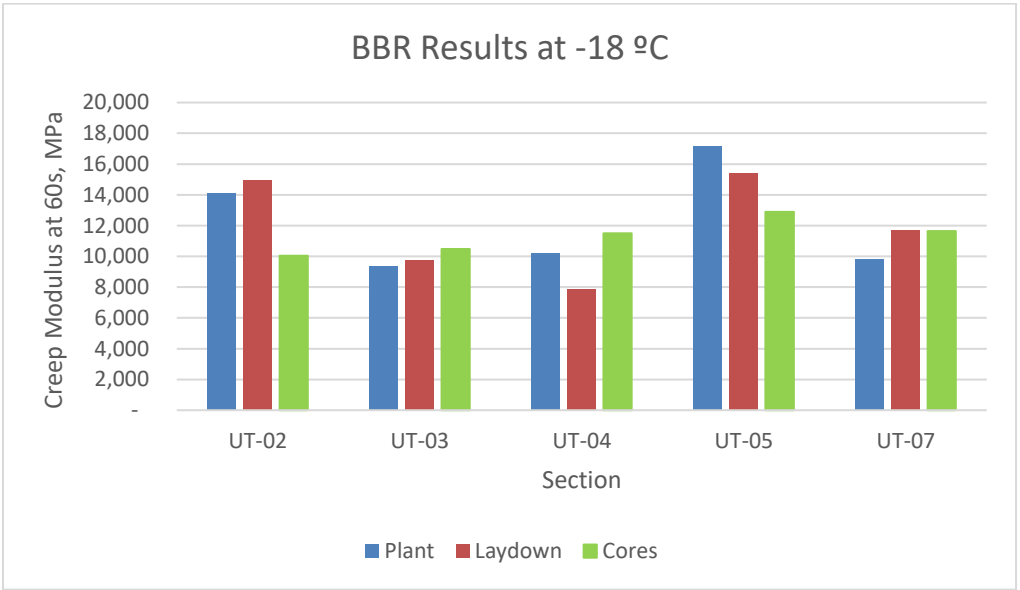

Figure 4-2 Comparison of Creep Modulus at -18 ºC

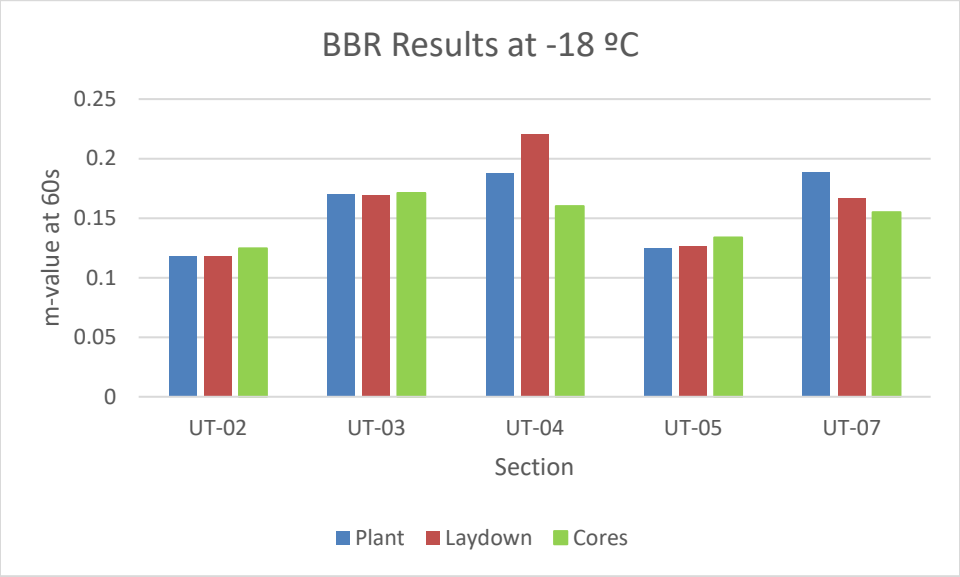

Figure 4-3 Comparison of m-value at -18 ºC

4.2.1.1 Discussion

The BBR test results obtained during mixing and compaction predict that UT-02 and UT-05 will likely show early thermal cracking. This is based on using a modulus of 12,000 MPa as the threshold and an m-value below 0.12. These sections have the highest RAP content and were designed using the Marshall method. However, this prediction is not captured from the tests done on cores; the results from the cores obtained from sections UT-02 and UT-05 actually show a decrease in creep modulus when compared to the values obtained during construction. While the decrease in creep modulus with aging seems counter intuitive, it is actually an indication of damage from microcracking. A detailed discussion on aging and microcracking is presented in Section 6.4 and actual microcracks can be seen in Figures 6-5 and 6-6.

Section UT-07 which only has 10% RAP content shows that the change in creep modulus between laydown and coring was negligible. At the same time, there is a trend of decreasing m-value from a high value of 0.19 to 0.15, but still above the 0.12 threshold value. Other sections (UT-03 and UT-04) showed a moderate increase in creep modulus with aging condition and a negligible change in m-value for UT-03 or a drop for UT-04. This illustrates how the effect of

aging can be reflected as an increase in creep modulus or a decrease in m-value. In asphalt binder, this is referred to as m-controlled or s-controlled material.

As was discussed in a previous UDOT report (Romero and VanFrank, UDOT Report No. UT-17.21, 2017), the effects of RAP blending and aging are mixture-specific, but the general trend of increased creep modulus and a decrease in m-value with aging and RAP is observed. This should be more apparent as more mixtures are tested. However, it is important to note that, for three of the five mixtures, the m-value remains above 0.15 indicating no significant loss in their ability to relax thermal stresses.

4.2.2 Comparison of Flexibility Index

The Flexibility Index, FI, obtained from the different mixtures at the different aging conditions is shown in Figure 4-4. The figure is based on the complete set of data from the cores (i.e., highest values not removed). The figure shows that sections UT-02 and UT-05 both have the lowest flexibility index values; these two sections are expected to show poor cracking performance based on FI values lower than 8. In all sections, the effect of aging is obvious since the FI value from 3-year old cores is lower than it was during laydown.

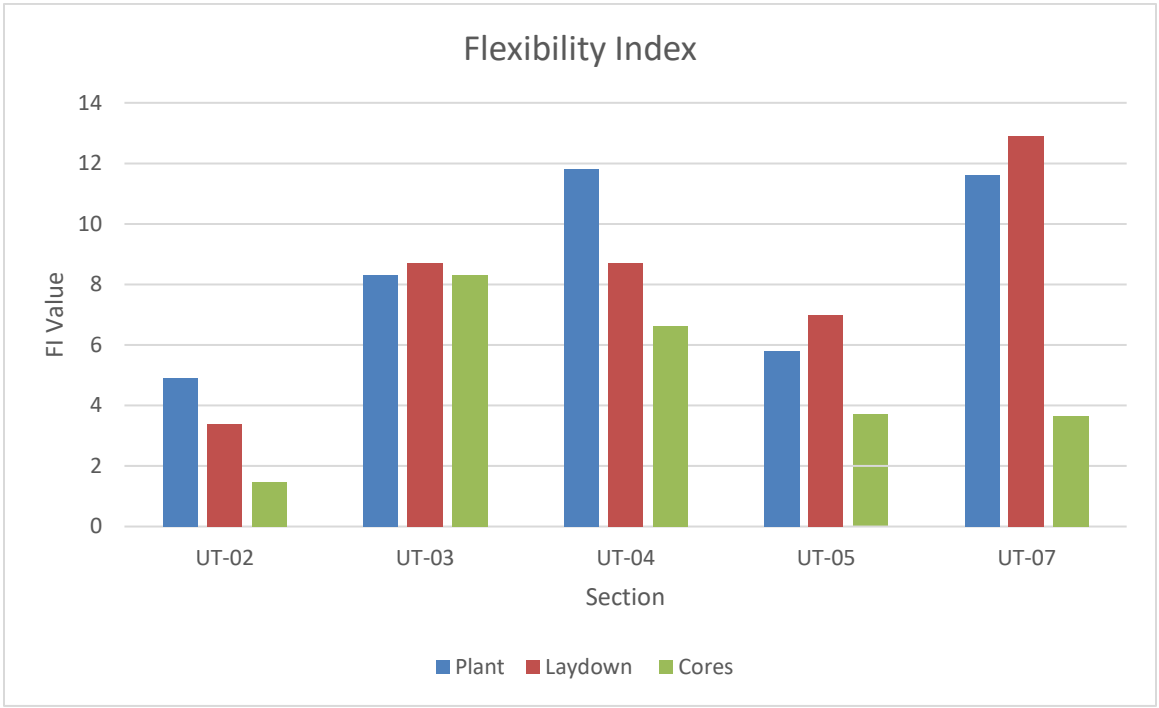

Figure 4-4 Comparison of FI Data at 25 ºC

4.2.2.1 Discussion

Figure 4-4 shows that there is a general trend of decreasing FI from the plant to laydown (short-term aging) and from laydown to cores (long-term aging). Regardless of the aging conditions, Section UT-02 is expected to have the worst performance of the group and using a threshold of 8 would also place UT-05 as a potential low performer. This is the same conclusion that was reached with the BBR results. These two mixtures were the only ones of the group designed following Marshall procedures and thus are not 'UDOT-type' mixtures.

Section UT-03 is the most consistent (i.e., no aging effects) with negligible changes in FI values across different aging periods. Similar results were also observed with the BBR. Section UT-07 had the highest FI during mixing and laydown, but had one of the lowest FI values in cores. It is hypothesized that the reason for such significant effect in aging might be related to its high virgin binder content; this will be explored in more detail in Section 6.3. The decrease in FI should be reflected in future performance.

It is also noted that those sections with low flexibility index also have high variability. As shown in Table 3-2, sections UT-02, UT-05, and UT-07 had coefficient of variation greater than 20% even after correcting for possible outliers.

4.2.3 IDEAL CT Data

As previously mentioned, during the 2017 study (2019 report), the IDEAL CT test was in the development process. This means that no CT Index on the construction data is available. However, since the publication of that study, The IDEAL CT test was selected by UDOT as the most likely candidate to evaluate intermediate-temperature performance.

The results from the cores are shown in Figure 4-5. In the same way as the other tests, the CT Index predicts that section UT-02 will have the worst performance of the group while section UT-03 is predicted to have the best performance of the group. However, unlike the two other tests, the CT Index shows section UT-04 as likely a poor performer and UT-05 should have better performance. This is the only test that predicts poor performance for section UT-04; the two other tests show a significant decrease in performance between laydown and coring.

The variability in the results is also very high for sections UT-02, UT-03, and UT-07 having coefficient of variation greater than 40%, while for sections UT-04 and UT-05 the variability is 11% and 6%, respectively. The performance of all sections will be discussed in Chapter 5.

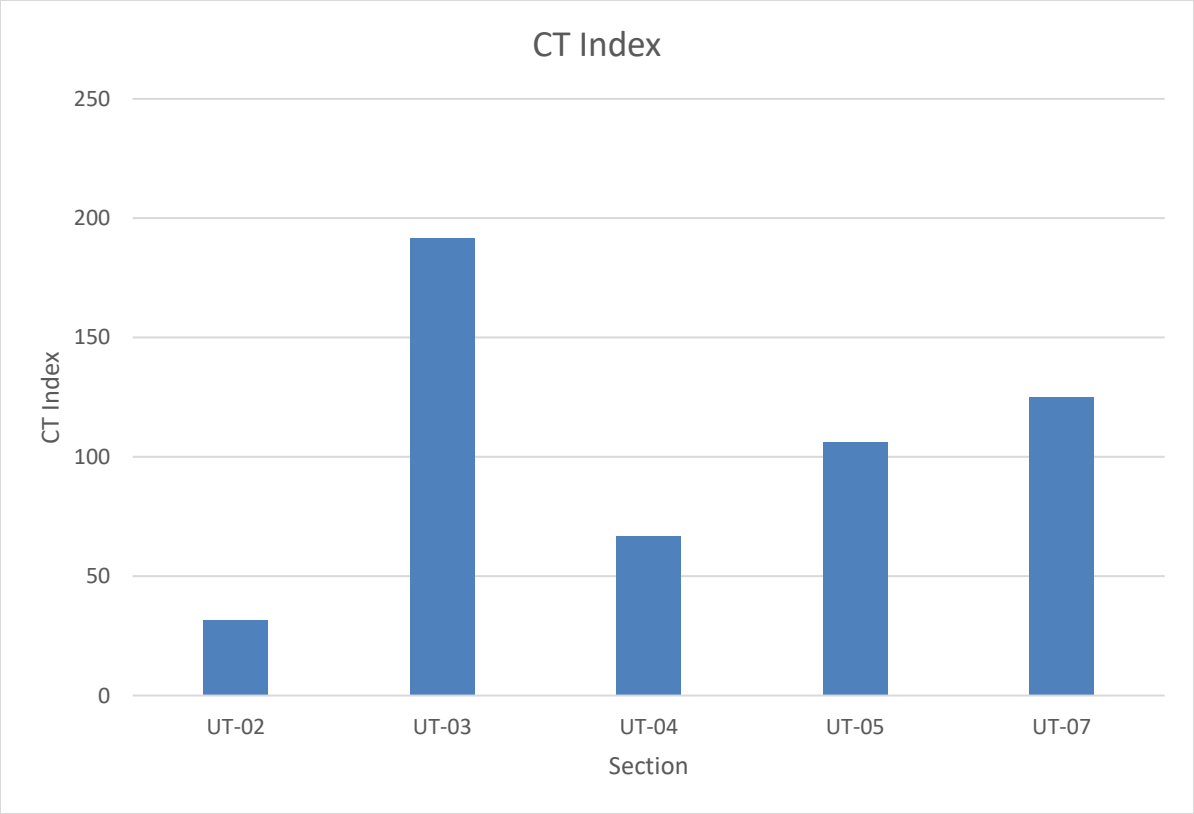

Figure 4-5 CT Index at 25 ºC

4.2.3.1 Comparison Between FI and CT Index

Given that there is no previous data for the CT Index to use as a reference, and to take advantage of the wealth of knowledge previously accumulated using the IFIT test, a relative comparison between the FI and the CT-Index was made. It is understood that the numbers would be different, but since both tests are based on similar concepts, it would be expected that a strong trend exists between them. The comparison between FI and CT Index is shown in Figure 4-6.

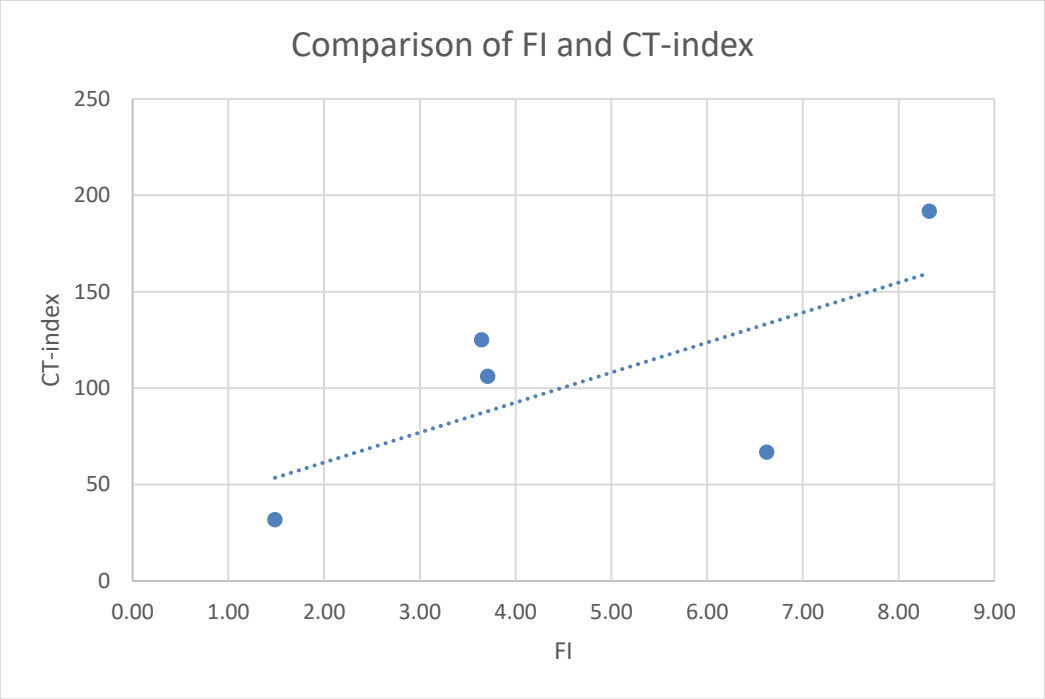

Figure 4-6 Comparison Between FI and CT-Index

Figure 4-6 shows that, for cores, the FI and CT Index have the same prediction for the best and worst expected performance; however, there is no agreement with intermediate performance predictions.

An alternative way to compare results between tests is shown in Table 4-1 in which the predicted best performing sections are shown. Similarly, Table 4-2 shows the predicted worst performers.

Table 4-1 Predicted Best Performers

2017 Lab Compacted		**2020 Cores**	
FI		**FI**	**CT Index**
Plant	Laydown		
UT-04	UT-07	UT-03	UT-03
UT-07	UT-03/04	UT-04	UT-07

Table 4-2 Predicted Worst Performers

2017 Lab Compacted		2020 Cores	
FI		FI	CT Index
Plant	Laydown		
UT-02	UT-02	UT-02	UT-02
UT-05	UT-05	UT-07	UT-04

Tables 4-1 and 4-2 show that there are differences among the tests in the prediction of the sections that are expected to perform well and the ones that do not. The only real commonality is that both FI and CT indices predict that section UT-02 should have poor performance. This holds true regardless of the aging condition evaluated.

4.3 Summary

Three different tests were performed on asphalt mixtures obtained during mixing and compaction and from cores after three years on the road. All tests predicted that section UT-02 would have poor performance. Both the BBR and the IFIT predicted that section UT-05 should have poor performance; one test based the prediction on the low m-value and the other one based it on the low FI. Looking at the data obtained from the cores, the FI predicts that after three more years, section UT-07 will start to deteriorate.

All three tests also predict that section UT-03 would have the best performance. There was, however, no agreement amongst the different tests for the ‘intermediate’ performing sections. It is not clear if index-type tests, such as the ones performed as part of this research, are meant for such fine-tuned predictions instead of providing pass-fail information.

5.0 PERFORMANCE OBSERVATIONS

5.1 Overview

While the field pavement sections were being cored, observations were made regarding the visible distresses on these sections. This chapter summarizes these observations and compares the performance predictions with the observed distresses.

5.2 Performance

For each section, the following performance was observed.

5.2.1 Section UT-02

This section is located in Tooele City, Skyline Drive, approximately 100 feet west of 200 East on the westbound travel lane (40°31'20.45"N 112°17'37.01"W). The pavement is not holding well; it shows sign of raveling and there is noticeable cracking observed in the section. This is shown in Figure 5-1.

Figure 5-1 Section UT-02 showing fatigue cracking and raveling

5.2.2 Section UT-03

This section is located in Randolph; approximately 1.5 miles south of Church Street on the southbound travel lane (41°38'37.16"N 111°11'0.34"W). Randolph is at an elevation greater than 6,200 feet, and it is worth noting that Rich County, where this is located, has often set low temperature records for the state of Utah. Therefore, it is not surprising that Figure 5-2 shows severe thermal and reflective cracking.

Figure 5-2 Section UT-03 Showing Thermal and Reflective Cracking

5.2.3 Section UT-04

This section is part of SR 32 in Kamas. It is in the 200 North eastbound lane, in line with the east sidewalk (40°38'46.93"N 111°16'50.26"W). The section shows some longitudinal joint opening but no other distress. This is shown in Figure 5-3.

Figure 5-3 Section UT-04 Showing Some Joint Opening

5.2.4 Section UT-05

This section is located in a subdivision in Provo at 3550 N 180 E (37° 5'51.50"N 113°33'18.63"W). The material was used as a patch and was sampled from a 17-hour old stockpile for custom sales. The small size of the patch makes any performance evaluation meaningless. A picture is shown in Figure 5-4.

Figure 5-4 Section UT-05 Used as Patch Material.

5.2.5 Section UT-07

This section is located on Heartstone Lane in Saratoga Springs, between Valkyries and School House (40°21'9.41"N 111°54'33.27"W). As shown in Figure 5-5, the road is part of a residential area and shows no visible distresses.

Figure 5-5 Section UT-07 Showing No Distresses

5.3 Summary

The observations described in this chapter confirm that, as predicted by all the tests during construction, section UT-02 did not perform well. As shown in Figure 5-1, this section had the most distresses after only three years of service. Section UT-05 was also predicted to have poor performance, yet no distresses were observed. However, given that it was used as a patch, actual distresses are difficult to assess.

Of interest is section UT-03. The overall prediction was adequate performance at intermediate temperature (high FI during construction), no thermal cracking at -28 ºC (creep modulus below 10,000 MPa and m-value above 0.17), but thermal cracking at -34 ºC (creep

modulus greater than 15,000 MPa and m-value of 0.12). As shown in Figure 5-2 the cracking predictions were accurate. There is significant thermal cracking even though the virgin binder used is listed as PG 64-34. This, once again, emphasizes the need for mixture testing rather than relying solely on one component.

Sections UT-04 and UT-07 were predicted to have good performance; no distresses were seen during the coring process, validating the predictions made during construction and given reasonable confidence in the ability of the tests to relate to performance.

6.0 EFFECT OF AGING

6.1 Overview

Previous chapters showed that aging plays a significant role in the results from mechanical tests. An asphalt mixture that might show adequate mechanical response during mixing and compaction might age significantly once placed in the field, resulting in potential failure from distresses. Section UT-07 is an example of such behavior showing significant changes between the original laydown mix and the 3-year old cores. Furthermore, sections UT-02 and UT-05 show a decrease in creep modulus after aging when tested in the BBR. This needs to be explained.

Long-term aging is mostly a chemical process; therefore, understanding how asphalt mixtures age from a chemical perspective and its relation with mechanical performance is a critical piece in creating a robust material specification. However, looking at field material is extremely complex as it is subjected not only to oxidation and UV degradation but also possible contamination from natural events such as acid rain and pollution as well as fuel and oil from traffic. Therefore, to better understand the chemical changes in asphalt mixtures as a result of aging, standard lab-prepared mixtures were used (instead of the field mixtures). Two mixtures, referred to as 'Mixture A' and 'Mixture B', are the standard mixtures previously used as part of this ongoing research. Both mixtures were made with the same PG 64-28 asphalt binder. Mixture A had a binder content by mass of 4.6%, a nominal maximum aggregate size, NMAS, of 19-mm, and limestone aggregate. Mixture B had a binder content of 5.3% by mass, a NMAS of 12-mm, and a blend of granite and quartzite aggregates. The details of these two mixtures can be found in UDOT Report No. UT-17.21 (Romero and VanFrank, 2017).

The samples were placed on the roof of the engineering building at the University of Utah. After three years on the roof (the same amount as the cores), two tests were used for the chemical analysis of the samples. One was the FT-IR spectrometry which provided the functional groups, and the other was the SEM-EDX which provided the topography and compositional contrast using secondary or backscattered X-rays.

6.2 Aging Study Samples

The mixtures were compacted in the lab and specimens for the BBR were cut. The BBR was selected since, unlike the other tests used in this research, it is non-destructive. It can test the same material multiple times. Ten beams were selected from each mix and placed on the roof of the Civil Engineering building at the University of Utah from Summer 2017 to Summer 2020. They were tested at regular intervals. At the end of the period, the samples were prepared for chemical analysis, and the results of this 'natural aging' were compared to the effects of extended oven aging. Natural aging is analogous to cores, while extended oven aging is meant as an accelerated aging conditioning process. The setup for natural aging is shown in Figure 6-1.

Figure 6-1 Picture of Beams Placed on the Roof to Evaluate Natural Aging.

6.3 FT-IR Analysis

6.3.1 Sample Preparation

After being conditioned, the samples were tested using FT-IR. The materials were ground using a mortar and pestle to increase the surface area and facilitate extraction of the binder using toluene. The mix was then filtered using Whatman 42 (2.5μm pore size) filter paper, and the filtrates were used for FT-IR spectrometry. The transmission mode in the FT-IR was used to obtain absorbance with a resolution of 4 cm^{-1} by averaging consequent 64 scans in the Nicolet iS50 FT-IR spectrometer.

6.3.2 FT-IR Functional Groups

The extracted aged binders with different RAP contents were analyzed using FT-IR with the results shown in Figure 6-2. Given that both Mixture A and Mixture B contain the same binder, only Mixture A is shown for clarity. The functional groups were identified using an FT-IR database (Beauchamp, P.Y., 2011).

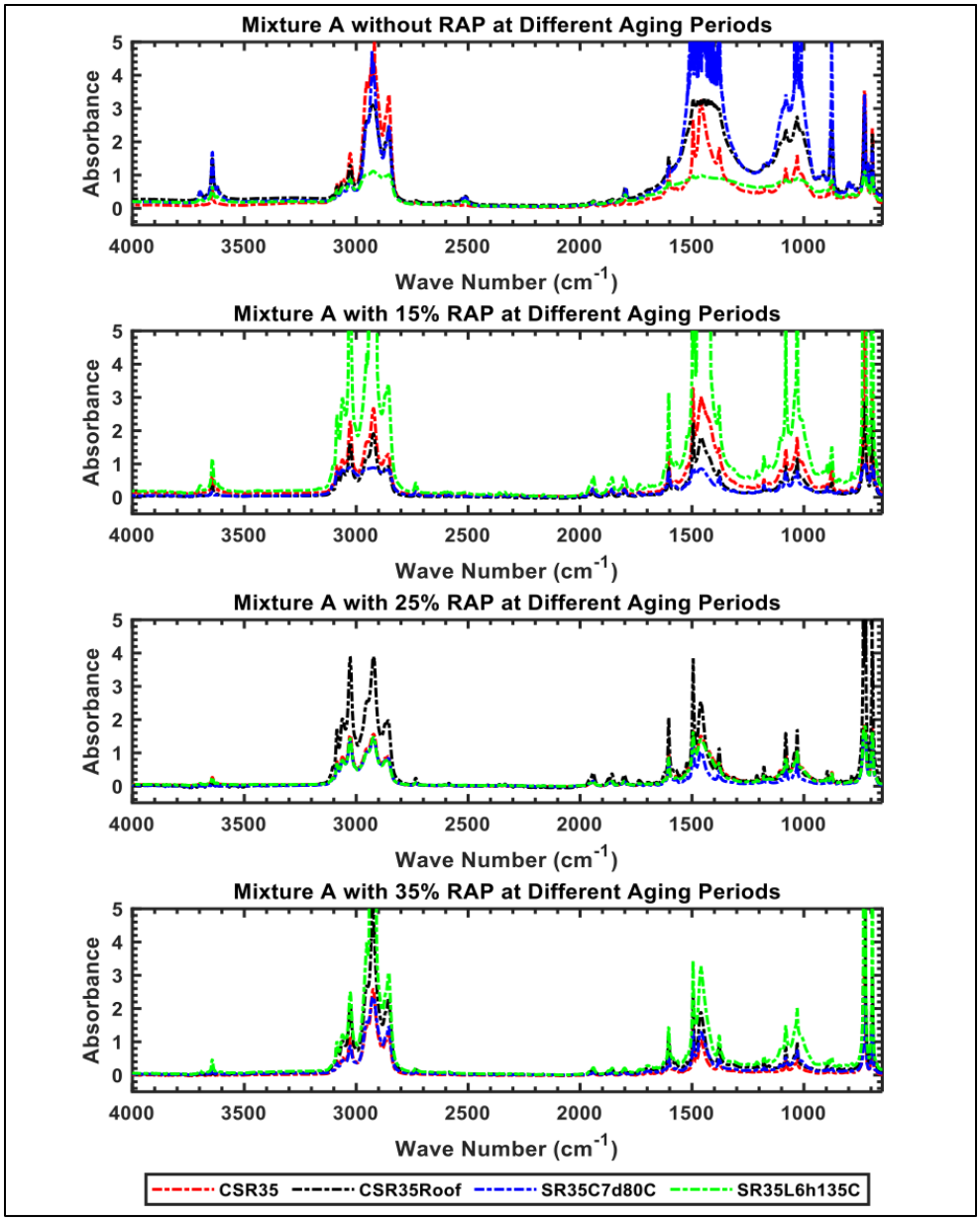

Figure 6-2 FT-IR Spectra of Mixture A with Different RAP Content

The black line represents natural aging, red line represents the baseline (no aging), the blue line represents oven aging of compacted samples and the green line represents oven aging of loose mix.

The band in between 2800 to 3000 cm^{-1} wavenumbers can be classified as typical sp^3 C-H bond stretching vibration (Beauchamp, P.Y., 2011). This band is insignificant in our context since all the specimens are expected to yield this band consisting of a significant proportion of aliphatic hydrocarbons. The same is true for the peaks observed at around 1600 cm^{-1} that can be attributed to the C=C bond in the benzene ring present in any polyaromatic hydrocarbons such as asphalt. An interesting pattern can be observed by looking at the peaks ranging from 3550 to 3650 cm^{-1}, where the peak heights and the areas under the peaks increased significantly with aging and RAP content. Similar patterns (i.e., peak height and area enhancement with aging) were observed within the 3050-3100 cm^{-1} and 1600-2000 cm^{-1} wavenumber range. The bands with aging can be correlated to the alcohol, acid, and carbonyl functional groups. All these functional groups contain oxygen that indicates the oxidation of hydrocarbon materials as a function of aging and the probable non-polar to polar transition of components due to the formation of oxygen-containing functional groups.

The intensity of a specific peak can be attributed to the sum of all contributions from all molecules containing a particular bond giving rise to that peak. The band area and peak heights were used to indicate the concentration of each functional group. Multiple band areas were investigated to isolate the effect of aging on asphalt binders by calculating the chemical bond index (I) as described in numerous publications (Yang et al., 2015; Lamontagne, et al., 2001):

$$I_{Alcohol} = \frac{AR_{3550-3650}}{\sum AR}$$

$$I_{Acid} = \frac{AR_{3050-3100}}{\sum AR}$$

$$I_{Carbonyl} = \frac{AR_{1600-2000}}{\sum AR}$$

Here, $AR_{3550\text{-}3650}$, $AR_{3050\text{-}3100}$, and $AR_{1600\text{-}2000}$ are the band areas in between 3550 and 3650, 3050 and 3100, and 1600 and 2000 cm^{-1}, respectively. $\sum AR$ is the cumulative area of all bands.

6.3.3 Correlation Between Physical Properties and Chemical Groups

The chemical bond index was plotted as a function of binder replacement by RAP for Mixtures A and B in Figure 6-3. The general trend of the chemical bond index is shown as a red-dashed line by considering all the differently aged samples' chemical indices. The general trend of increasing stiffness (creep modulus) obtained from the BBR tests of those corresponding variants with different RAP contents is plotted as a black-dashed line. Only the major functional groups' chemical indices are shown to avoid cluttering.

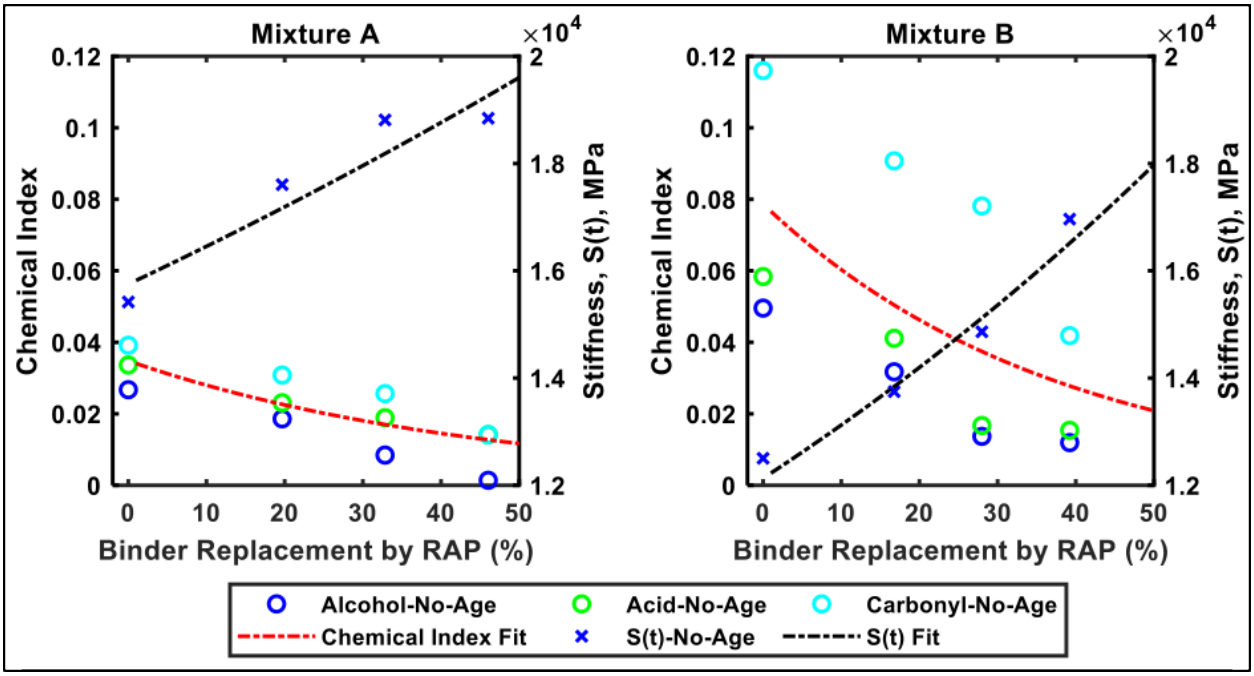

Figure 6-3 Chemical Bond Index as a Function of Binder Replacement for Major Groups

Looking at Figure 6-3, it is readily observable that stiffness is inversely correlated with the chemical bond index; stiffness increases with RAP content while the bond index decreases (i.e., red and black lines have opposite slope). Since the chemical bond indices mainly appraise the oxygen-containing functional groups, the increase in BBR specimens' stiffness can be envisaged as a function of asphalt oxidation.

The higher chemical bond index at lower RAP percentage suggests concentrated functional groups that decrease with RAP percentage. The behavior seems contradictory: Mixtures with higher RAP contents should have higher chemical bond indices with higher aged

and oxidized asphalt contents. Two factors were considered to explain this conflicting behavior: asphalt oxidation stages and diversity in asphalt molecular formula.

Asphalt oxidation is dominated by different mechanisms at different stages of oxidation. Typically, the first oxidation process happens to the molecules with heteroatoms that are polar and can easily interact with oxygen. At the second stage, the benzylic carbon of asphalt molecules possibly starts to interact with oxygen to yield ketonic compounds. If multiple benzylic carbons are present, then an acidic anhydride might be formed (Dorrence et al., 1974). These reactions are highly governed by iron and manganese salts from the inorganic aggregates in pavements. A higher proportion of ferric chloride or manganese oxide can increase the reaction rate significantly. The complex bi-stage reactions can eventually yield two different types of products: (1) molecules with no change in carbon number and (2) molecules with varying carbon numbers. The latter case is prominent if the asphalt molecules consist of a high proportion of alkyl side-chains capable of undergoing cleavage during oxidation and yield smaller molecules and volatiles (e.g., CO_2) easily escapable to the environment. The diversity of asphalt molecules is, therefore, vital as it dictates the products of the oxidation. Asphalt molecules with a high proportion of heteroatoms and alkyl side-chains are more likely to spawn smaller molecules and volatiles that typically escape to the atmosphere at ambient temperature.

BBR specimens with higher RAP content contained a higher proportion of already aged asphalt molecules, thereby reluctant to further oxidation with a lower number of heteroatom(s) or alkyl side-chains. The concentration of functional groups, observable in Figure 6-2, is lower than the specimens with higher virgin asphalts. The behavior can be observed more clearly when non-aged specimens are considered without any effect of age-hardening, as shown in Figure 6-3.

The control mixtures were exposed to two hours of oven aging before compaction to simulate the field paving according to AASHTO T312; therefore, it is safe to consider the aging effect as insignificant. The chemical bond index at 0% RAP content can be attributed to the naturally occurring functional groups (e.g., 2-quinolone, phenol) in the virgin asphalt molecules (Petersen, 2009). Since the proportion of virgin asphalts decreases with increasing RAP percentage, each bond's average concentration decreases to reduce the chemical bond indices.

Different chemical indices for Mixture A and B demonstrate the difference in molecular structures of asphalt molecules obtained from two distinct sources.

However, the increasing amount of RAP binder did not increase the chemical bond index. This is consistent with toluene being able to only dissolve the virgin-binder portions while the highly oxidized RAP fractions could be toluene-insoluble and filtered out. While this explains the inverse relationship between stiffness and virgin binder replacement by RAP, further research on extracting RAP binder with a different solvent is necessary.

6.4 SEM Analysis

6.4.1 Sample Preparation

To prepare samples for the SEM-EDX analysis, each beam was trimmed into approximately 12.7 mm x 12.7 mm x 2 mm samples using a wet-tile saw. The samples were then rinsed and sonicated to remove any debris. Once the specimens were dry, they were placed on a stage dedicated to the specific SEM-EDX model (Hitachi TM3030 Plus). A double-sided copper tape was used to attach the sample to the stage and ensure electron conductivity. The setup is illustrated in Figure 6-4.

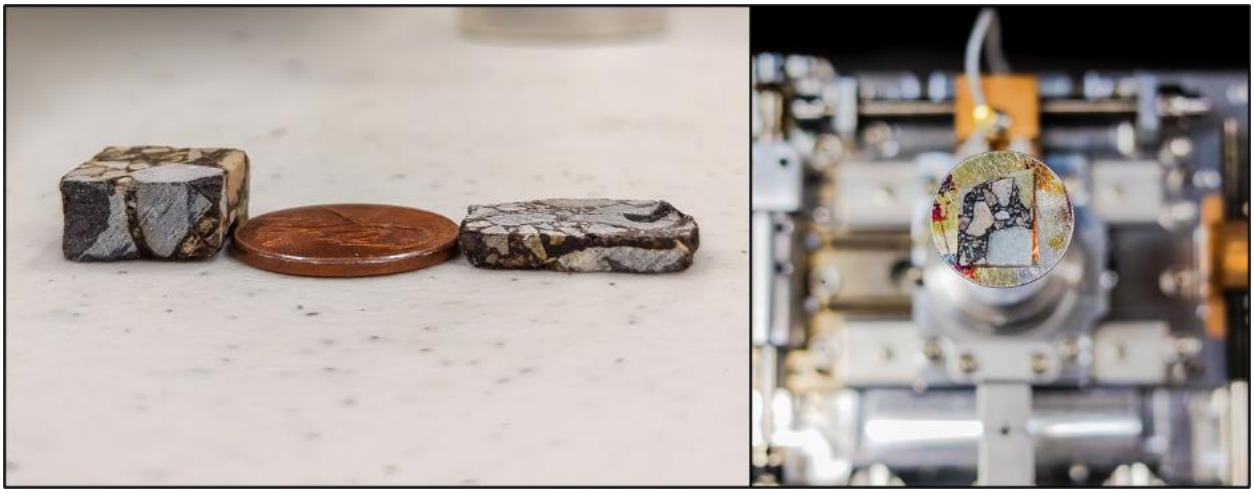

Figure 6-4 Sample for SEM-EDX Analysis
On the left, the penny is used for reference; on the right, the sample is attached with copper tape

6.4.2 SEM Topography

The standard testing protocol for the Hitachi TM3030 Plus was followed for conducting all the analyses. The SEM's EDX function was used with an electron landing energy of 15keV over a 500μm sample surface area at 200x magnification. Although an asphalt mixture is a heterogenous and viscoelastic material that contains both organic and inorganic materials, the captured images of surfaces had approximately 50-50 distribution between asphalt mastic (binder and fine aggregates) and coarse aggregates. This visual approximation can be ensured by measuring the relative composition of elements over the scanned surface of the specimen. A total of 12 samples were used to analyze its topography and elemental composition using the BSE function on the SEM-EDX.

The BSE images of the asphalt mixture samples' topography are shown in Figure 6-5 for Mixture A and Figure 6-6 for Mixture B. The numbers within each image represent the data ID, date and time, focus, magnification, and image area length, respectively (from left to right).

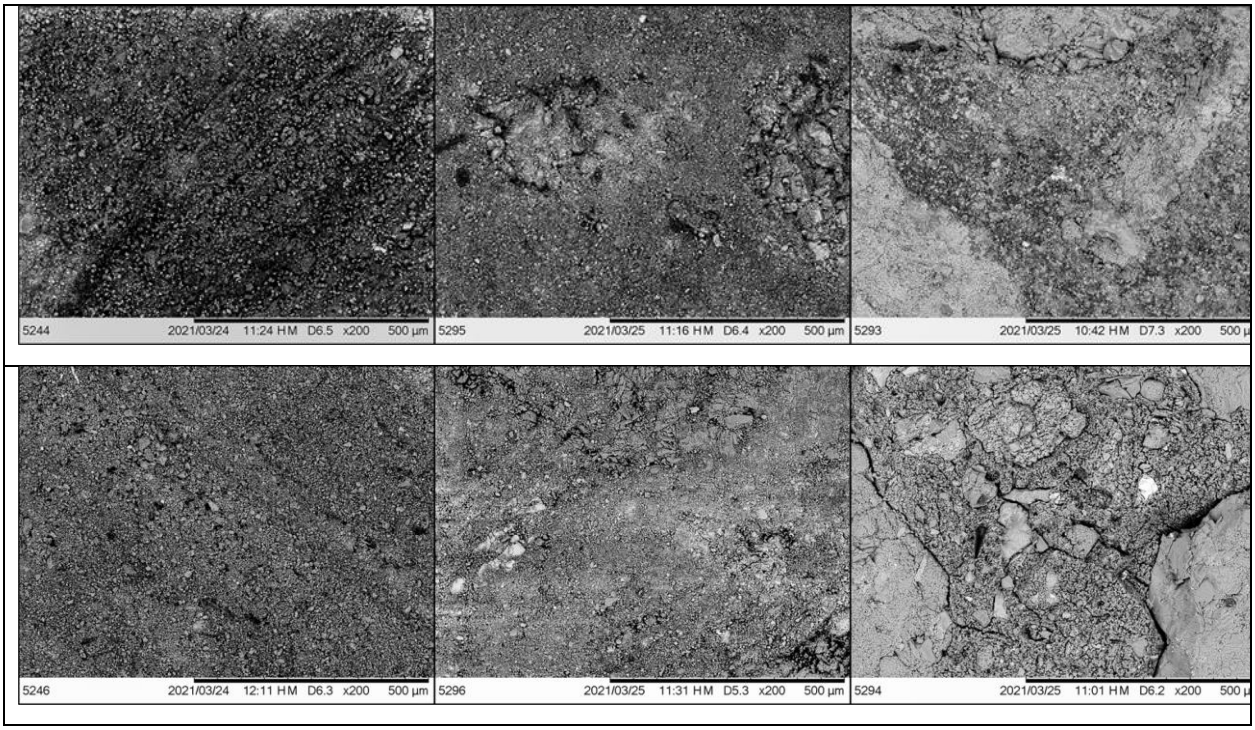

Figure 6-5 Topography of Mixture A with 0% RAP (Top) and 35% RAP (Bottom)

Left to right: control, 6-hour oven aged, naturally aged

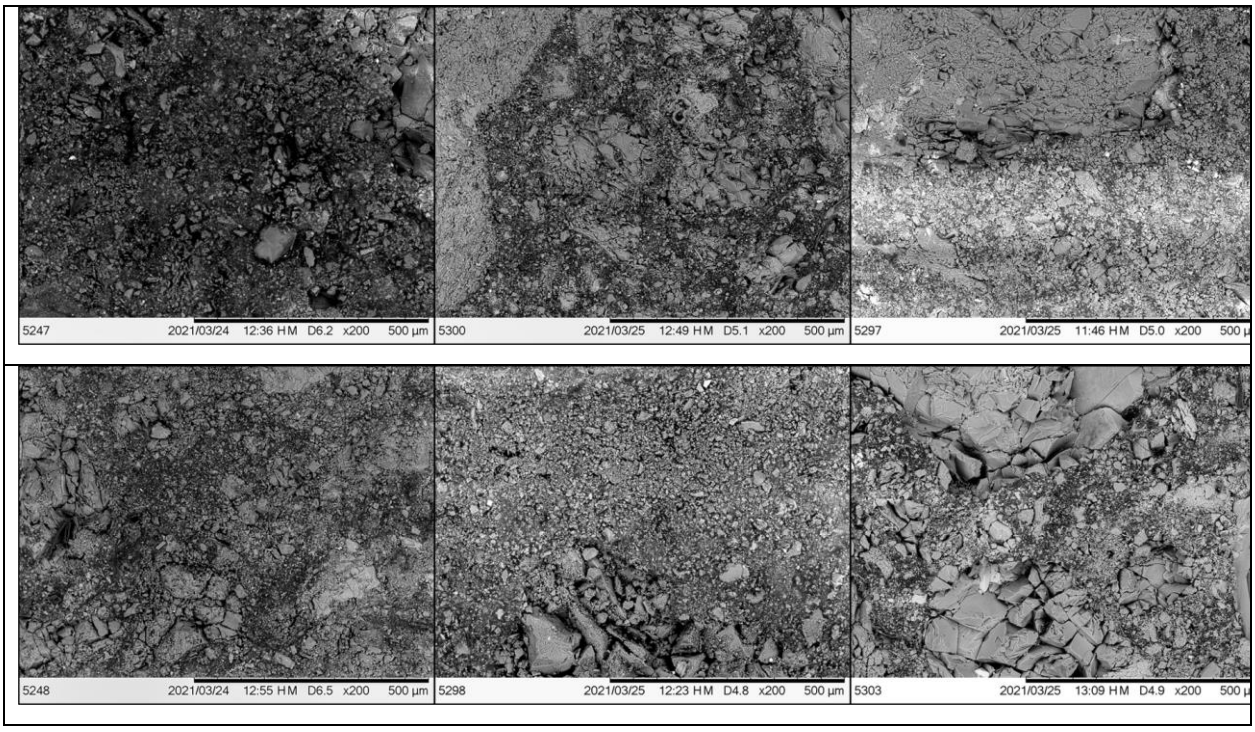

Figure 6-6 Topography of Mixture B with 0% RAP (Top) and 35% RAP (Bottom)

Left to right: control, 6-hour oven aged, naturally aged

Overall, it is apparent that as asphalt concrete ages, it loses organic compounds through volatilization, and then the samples turn greyer or brighter with increasing RAP content and aging periods. Mixture A samples show higher contrast than Mixture B samples. Organic compounds in asphalt mixture are primarily hydrocarbons (low atomic numbers), and aggregates are mostly compounds of calcium, aluminum, and silicon (high atomic numbers). So, the high average atomic number regions appear brighter than regions of low atomic number (Abdalfattah, et. al., 2021). This finding is consistent with the FT-IR discussion in Section 6.3. The formation of volatiles such as CO_2 and ketones was mentioned with high RAP content and aging periods.

Additionally, the air voids appear as black holes on the BSE topography. As the aging period increases, the surface texture appears rougher by losing organic components, and the inter-particle voids extend within the sample. Especially for the naturally aged sample for Mixture A with 35% RAP, it is observed that the voids are interconnected to make a microcrack around the interface between asphalt mastic and coarse aggregates. This appearance of microstructural damage is a direct result of high RAP content and extensive aging. This asphalt mixture's stiffness was also the highest among all variants (S = 26,340 MPa, *m*-value = 0.103).

While there is still no sign of microcrack on the similar variant of Mixture B (S = 24,450 MPa, *m*-value = 0.096), the sample is likely to form cracks with further aging. High RAP content and excessive aging contribute to the microcracks' formation and lead to macrocracking at low temperatures. This helps explain the behavior for mixtures UT-02 and UT-05 shown in Figures 4-2 and 4-3 in Section 4.2.1.

The elemental analysis can also demonstrate the loss of organic elements. The primary electrons and the sample surface interact with each other, which leads to the emission of X-rays. EDX allows for capturing the energy dispersed by the secondary electrons and makes it possible to identify the elements present on the sample surface. It also maps the relative distribution and concentrations of previously defined elements over the scanned area. The atomistic distribution over the scanned surface is tabulated in Tables 6-1 and 6-2. It demonstrates the relative concentrations of elements present in the samples.

Table 6-1 Molecular Percentage of Elements by Weight for Mixture A

Element	Control	6-hour oven aged	Naturally aged	35% RAP	35% RAP, 6-hour oven aged	35% RAP, Naturally aged
C	16	10	4.6	6	8.4	4.4
O	31.1	34	36.5	30.7	43.6	44.1
Na						
Mg	1.5	1.5	1.3	2.6	4.4	7.4
Al	2.1	1.5	0.9	2.2	4.7	3.5
Si	4.9	4.8	4.4	7.1	7.6	14.4
S	4.2	2.4	1.1		1.9	0.6
K	0.5	0.5	0.4	1.7	1.5	1.5
Ca	39.8	45.2	50.7	49.8	27.1	20.8
Fe					0.7	3.4
Mo						

Table 6-2 Molecular Percentage of Elements by Weight for Mixture B

Element	Control	6-hour oven aged	Naturally aged	35% RAP	35% RAP, 6-hour oven aged	35% RAP, Naturally aged
C	25.1	13.1	8.3	18.9	7.1	3.2
O	29.2	18.2	37.6	33.4	13.4	43.2
Na	0.4		0.6	0.4		
Mg	0.8	1.5	0.7	1.5	0.6	
Al	3.3	6.1	2.4	2.9	18.2	1
Si	30.4	25.6	40.9	32	42.3	51.4
S	2.8	8.1		2.2	1.4	
K	1.2	3.3	0.7	0.9	13.1	0.6
Ca	4.8	10.7	4.4	6.2		0.6
Fe	1.9	13.5	2.1	1.7	4	
Mo			2.4			

Only 11 elements constituted 100% of the scanned surface in the SEM-EDX. Hydrogen and helium cannot be detected using SEM-EDX, which is a limitation for detecting hydrocarbons using this analysis. Some of the molecules, such as sodium and molybdenum, were present in trace amounts. Also, iron and sulfur were present in some of the variants. Sulfur concentration decreases with increased RAP and aging due to sulfoxide formation. The source of iron could be attributed to the RAP aggregates.

However, it must be noted that each specimen has its unique distribution and random aggregate structure. Therefore, the scanned area is an arbitrary representation of the mixture characteristics. Both asphalt mastic (binder and fine aggregates) and coarse aggregates deserve representation in the microscopy. In Tables 6-1 and 6-2, the elements that are predominantly present in the coarse aggregates (Ca, Si, Fe, Al, etc.) constitute less than 60% of the scanned surface confirming the visual approximation of keeping the scanned area of the mixture specimen at 50-50 distribution between the asphalt mastic and coarse aggregates.

Additionally, the carbon concentration is inversely correlated with increasing RAP and aging. The oxygen concentration mainly increased with RAP and aging. The carbon concentration is the lowest in naturally aged samples, whereas the oxygen content is the highest in the same environment. This is consistent with the observation that the hydrocarbon within the asphalt mixture gets oxidized with time until a certain point when its concentration becomes too low to react anymore. The behavior can be observed more clearly if the C/O ratio is considered, as shown in Figure 6-7. The C/O ratio is higher for the control mixture, but the ratio starts to fall with aging since the aromatic carbons get oxidized and some of them escape to the environment. With lower C/O ratio, the specimens become brittle and cannot release stress during shrinkage at low temperature (high stiffness, low *m*-value), hence forming microcracks. Thus, the results from SEM-EDX validate the interpretation of the qualitative data obtained from the FT-IR spectral analysis. Additionally, investigating the C/O ratio eliminated the influence from variations in the amount of binder vs. aggregate in the SEM micrographs.

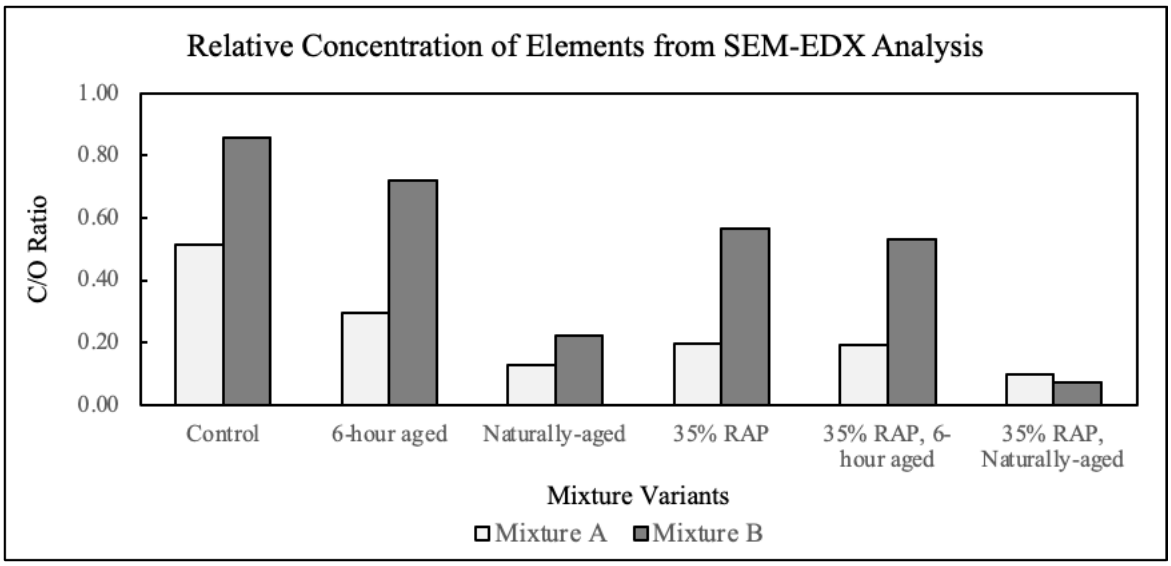

Figure 6-7 C/O Ratio of the Scanned Surface

Another significant advantage of using SEM-EDX is that it provides the percentage of the inorganic molecules. As the aggregates of Mixture A came from a limestone quarry, it shows a high concentration of calcium in the samples. Aggregate for Mixture B came from granite and quartzite quarries; granite and quartzite are igneous rocks, mainly composed of alumino-silicates and other metallic compounds. Therefore, the concentration of aluminum and silicon is higher

than in Mixture A. The relative distributions of elements within the scanned area can also be demonstrated using a mapping from the BSE analysis shown in Figure 6-8.

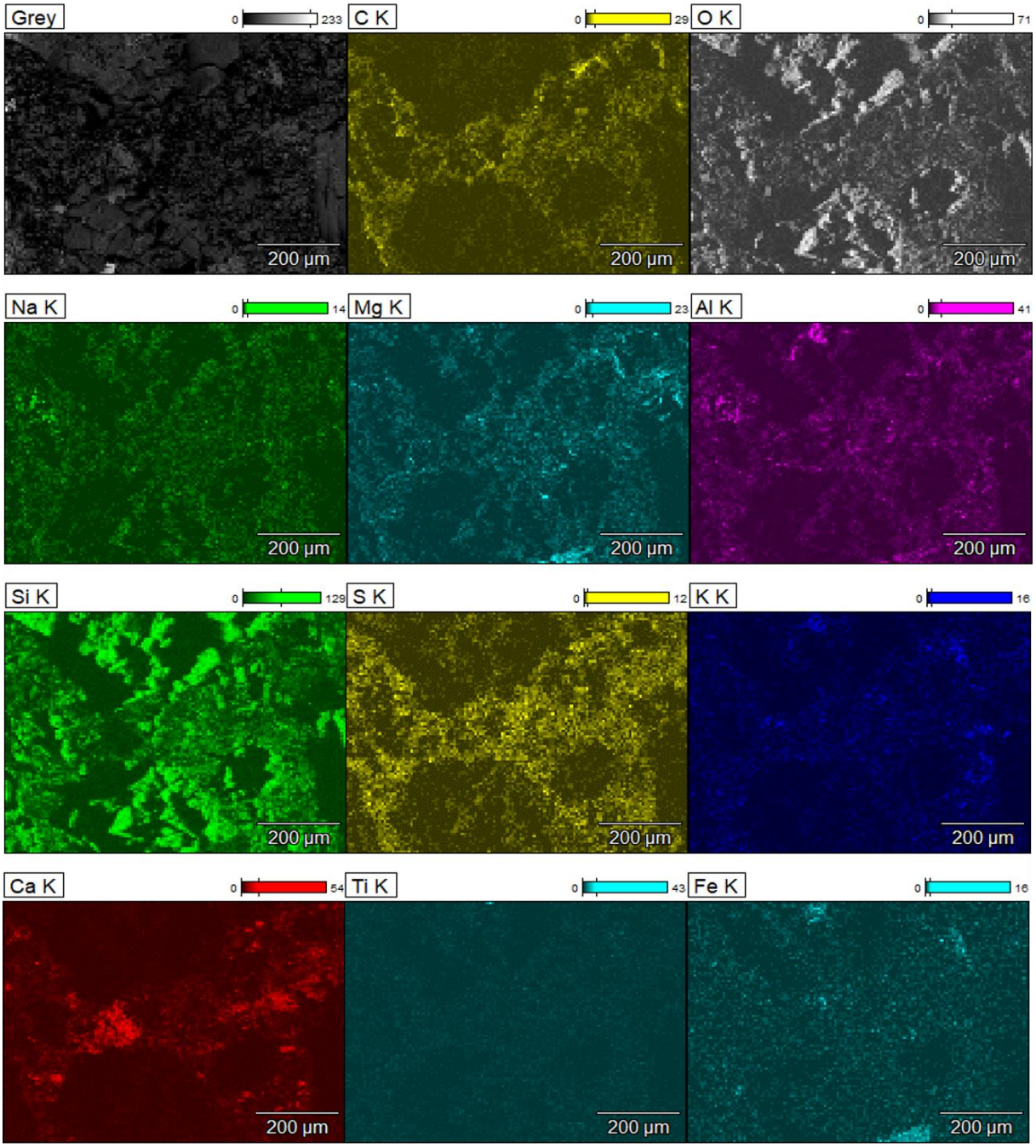

Figure 6-8 Relative Distribution of Compositional Elements Within Mixture B
Obtained using SEM-EDX analysis of Mixture B, 35% RAP, 3-year aged naturally

Figure 6-8 represents a map of the elements present in Mixture B with 35% RAP that was aged outside for three years (a condition analogous to the cores discussed in Chapter 3.0). In general, carbon, calcium, and sulfur are part of the asphalt mastic, whereas silicon and aluminum are dominantly present in the coarse aggregates. As 1% lime was added to the mixture as an anti-stripping agent, the calcium in the mastic represents that lime. Oxygen maps the voids over the scanned surface. Trace amounts of titanium and iron are present too; they might have come from air pollution. Small amounts of sodium and magnesium could have come from the atmosphere through precipitation and the minerals within aggregates.

Overall, the topography, elemental analysis, and mapping of the elements make the SEM-EDX an excellent tool to analyze the chemical composition of asphalt mixtures and its relation with the material properties and observed performance. These findings are valid for the specific materials analyzed in this study; different sources of materials could produce different results.

6.5 Summary

In order to better understand the changes that occur in the field, thin-beam specimens made with standard asphalt mixtures were aged in a controlled outdoor environment for three years. This provided an insight into the chemical changes that asphalt mixtures can undergo while in the field and relate them to the observed behavior. Based on the analysis, it was found that mixtures with high virgin binder content might result in low stiffness when measured in fresh mix but can oxidize faster than mixtures containing RAP binder, demonstrating the need to characterize the material in the appropriate aged state.

The FT-IR was used to identify the functional groups produced in the asphalt mixtures due to oxidative aging. Three critical chemical groups were identified using an area-integral method from the FT-IR spectra: acids, carbonyls, and alcohols. The observations were validated using the SEM-EDX analysis. When too much loss of organic molecules occurs within the mixture, asphalt mastic loses cohesion with the aggregates and becomes brittle. At low-temperature, it loses its relaxation properties and forms microcracks which might result in a reduction in stiffness with aging leading to the wrong conclusion regarding low-temperature performance.

7.0 CONCLUSIONS

7.1 Summary of Results

The objectives of this research were to evaluate the performance of pavement sections constructed from mixtures previously evaluated and then determine the effect of field aging based on cores obtained from these pavement sections. The purpose of such testing was to determine if a single value from mechanical testing such as the FI or the CT Index relates to field performance in terms of pavement cracking at intermediate temperatures. It also serves as validation of previous work regarding the BBR testing of mixtures.

Using the information presented in this report, a threshold or limiting value for a cracking index at intermediate-temperature cracking based on the observed pavement condition and considering the aging of the material is proposed.

Finally, the effects of aging and the chemical changes resulting from long-term oxidation are presented and related to the observed mechanical properties.

7.2 Findings

The most relevant findings from this work are summarized in this chapter.

7.2.1 Performance Testing

The data obtained as part of this work shows that the CT Index obtained from the IDEAL CT at 25 ºC can identify mixtures with potential for premature failure the same way as the FI obtained from the IFIT. This means that the test can be used to detect potentially problematic mixtures, as was shown in Chapter 5.0. However, it is recognized that the CT Index and the FI are pass/fail values. There is not enough information from this work to determine the validity of the tests to predict performance beyond this pass/fail determination. Mixtures that had acceptable cracking indices showed no distresses; no inference is made beyond that statement. In other words, there is no evidence that a material with very high flexibility index (or CT Index) would result in better performance than a material with an acceptable index (i.e., a value higher than the

threshold). Information on a large number of pavement sections over a longer period of time would be needed to make such a determination.

At low temperatures, the BBR on mixtures, once again, showed that it can identify asphalt mixtures that might show thermal cracking. These predictions are specific to the environment in which the material will be placed.

7.2.2 Threshold Values

There has been significant testing done on the Flexibility Index. Based on the overall volume of work, including previous research and data presented as part of this report, mixtures with an FI less than 8 are considered susceptible to early fatigue cracking and should be avoided. Therefore, an FI value greater than 8 on mixtures compacted after short-term aging should be used as a threshold value.

Using the imperfect relation shown in Figure 4-6, and using an FI value between 6 and 8 as a threshold, a CT Index of 125 to 150 was estimated to be the minimum acceptable value for mixtures compacted in the lab with no long-term aging. Given that all of the tested mixes were developed using the Hamburg Wheel Tracker as the only performance test, more testing on a wider range of mix designs is required to narrow the value. It is also clear that since the IDEAL-CT test is performed at a single temperature and displacement rate, different index values must be set for different temperature environments.

For low-temperature cracking, a stiffness (creep modulus) less than 12,000 MPa and an m-value greater than 0.12 at the temperature related to the expected environment is found to be the appropriate threshold. Previous research has shown that adequate performance can be achieved with higher stiffness values as long as the m-value also increases; however, no research has shown adequate performance in mixtures with an m-value below 0.12. See UDOT Report No. UT-16.09 by Romero, for more information regarding BBR testing.

7.2.3 Effect of Aging

This work demonstrated a clear relation, based on both chemical and mechanical testing, between field long-term aging and the increase in creep modulus and decrease in relaxation

capacity of asphalt mixtures at low temperatures. Aged mixtures also show increased microcracking that can result in an apparent reduction in creep modulus at low temperatures. At intermediate temperatures, a reduction in flexibility with field aging was also observed.

Mixtures with more virgin binder can be more reactive to oxidation and should be evaluated based on extended laboratory aging. Higher CT Index values might be used to compensate for aging phenomenon and result in pavements with longer life.

7.3 Conclusions

Based on the results obtained as part of this project, it is concluded that the proposed mechanical testing at low and intermediate temperatures can be used to identify mixtures that might have poor cracking performance in the field. Tests at low and intermediate temperatures can be used during the mix design process to prevent poor-performing mixtures from being placed in the field.

7.4 Limitations and Challenges

The findings of this research are limited to the specific pavement sections evaluated under the specific testing conditions. A larger database can provide more precise information regarding the relation between mechanical testing and pavement performance. However, even with more data, the general conclusions are expected to hold since they are also based on mechanistic principles.

8.0 RECOMMENDATIONS AND IMPLEMENTATION

8.1 Recommendations

It is recommended that UDOT adopt the IDEAL CT tests as a requirement for asphalt mixtures during design. A CT Index value of 125 to 150 was estimated to represent a preliminary threshold to prevent premature failures. The material should be conditioned for short-term aging since, even at that condition, enough information is obtained to make an assessment. In cases where there is doubt due to test results being close to the threshold, the loose asphalt mixture can be conditioned in the oven for longer times to simulate the long-term aging conditioning prior to compaction and then re-tested.

It is recommended to continue the implementation of the BBR in mixtures as a test to evaluate the asphalt mixture potential for low-temperature cracking. Part of the specification should include the condition that if an aged material shows a decrease in stiffness or increase in m-value, that material should be rejected since such decrease in values is the result of microcracking.

8.2 Implementation Plan

A specification for low- and intermediate-temperature testing of asphalt mixtures during the design phase should be adopted. Testing should be done for information only during the first year or two to gather needed data, and then it should be adopted as a statewide requirement. Continued training and education in all asphalt mixture laboratories of both users and producers should be conducted to ensure consistent results.

REFERENCES

AASHTO Provisional Standard TP124: Standard Method of Test for Determining the Fracture Potential of Asphalt Mixtures Using the Illinois Flexibility Index Test (I-FIT), American Association of State Highway Transportation Officials, Washington, DC (2016)

AASHTO Provisional Standard TP 125: Standard Method of Test for Determining the Flexural Creep Stiffness of Asphalt Mixtures Using the Bending Beam Rheometer (BBR). American Association of State Highway Transportation Officials, Washington, DC (2016)

Abdalfattah, I.A., Mogawer, W., and Stuart, K: *Quantification of the degree of blending in hot-mix asphalt (HMA) with reclaimed asphalt pavement (RAP) using Energy Dispersive X-Ray Spectroscopy (EDX) analysis*. Journal of Cleaner Production Volume 294 (2021) https://doi.org/https://doi.org/10.1016/j.jclepro.2021.126261

Asib, ASM., Romero, P., and Safazadeh, F.: *Number of Replicate Beams Required for a Valid Test of Asphalt Mixtures Using the Bending Beam Rheometer Based on AASHTO TP125*. Paper 18-01626 presented at the Transportation Research Board 97th Annual Meeting, Washington DC (2018)

ASTM D8225-19: Standard Test Method for Determination of Cracking Tolerance Index of Asphalt Mixtures Using the Indirect Tensile Cracking Test at Intermediate Temperature. American Society of Testing and Materials, Philadelphia, PA (2019) http://www.astm.org/cgi-bin/resolver.cgi?D8225

Beauchamp, B. P.Y.: Spectroscopy Tables 1, Organic Chemistry 2620 A-16, A17. (2011) http://www.cpp.edu/~psbeauchamp/pdf/spec_ir_nmr_spectra_tables.pdf .

Dorrence, S.M., Barbour, F.A., and Petersen, J.C: *Direct evidence of ketones in oxidized asphalts*. Analytical Chemistry Vol 46 Pp 2242–2244. (1974) https://doi.org/10.1021/ac60350a003

Ho, C.H. and Martin Linares, C.P.: *Determining the Number of Specimens replicates in support of pavement construction using AASHTO TP125*. Journal of Transportation Engineering, Part B: Pavements. Volume 145 Issue 2 (2019) https://doi.org/10.1061/JPEODX.0000109

Jones, Z., Romero, P., and VanFrank, K.: *Development of low-temperature performance specifications for asphalt mixtures using the bending beam rheometer*. Journal or Road Materials and Pavement Design. Volume 15 Issue 3 (2014) https://doi.org/10.1080/14680629.2014.908135

Lamontagne, J., Dumas, P., Mouillet, V., and Kister, J.: *Comparison by Fourier transform infrared (FTIR) spectroscopy of different ageing techniques: application to road bitumens*. Fuel. Volume 80 Issue 4 Pp 483–488. (2001)

Petersen, J.C.: *A review of the fundamentals of asphalt oxidation: chemical, physicochemical, physical property, and durability relationships*. Transportation Research Circular Number E-C140 (2009).

Romero, P.: *Using the Bending Beam Rheometer for Low Temperature Testing of Asphalt Mixtures*. UDOT Report No. UT-16.09. Utah Department of Transportation, Salt Lake City UT (2016) https://drive.google.com/file/d/16J9AApBJBxVQdY-sNFxWJFgEEYLB-_S0/view

Romero, P. and VanFrank, K.: *Balanced Asphalt Concrete Mix Performance, Phase II: Analysis of BBR and SCB-IFIT Tests*. UDOT Report No. UT-17.21. Utah Department of Transportation, Salt Lake City UT (2017) https://drive.google.com/file/d/1yf5b2zn-IV58zZL5UzgcUl6lxUqbJm0G/view

Romero, P. and VanFrank, K.: *Balanced Asphalt Concrete Mix Performance in Utah, Phase III: Evaluation of Field Materials Using BBR and SCB-IFIT Tests*. UDOT Report No. UT-

19.15. Utah Department of Transportation, Salt Lake City, UT (2019) https://drive.google.com/file/d/10NBODLBPlfIZJ0tDDY5baRNF_zFqaU9Y/view

Safazadeh, F., Romero, P., Asib, ASM., VanFrank, K.*: Practicality of Driven Parameters of Semi-Circular Bending Tests at Intermediate Temperature*. Journal of Transportation Engineering, Part B: Pavements. Volume 147 Issue 3 (2021) https://doi.org/10.1061/JPEODX.0000284

VanFrank, K. and Romero, P.: *Balanced Asphalt Concrete Mix Performance in Utah, Phase IV: Cracking Indices for Asphalt Mixtures*. UDOT Report No. UT-20.13. Utah Department of Transportation, Salt Lake City, UT (2020) https://drive.google.com/file/d/1R67M-Lt5R2I0-mdEcnhGfq6vkJDhZkna/view

Yang, X., You, Z., Mills-Beale, J: *Asphalt binders blended with a high percentage of biobinders: Aging mechanism using FTIR and rheology*. Journal of Material in Civil Engineering 27 (2014) https://doi.org/10.1061/(ASCE)MT.1943-5533.0001117

APPENDIX A: Flexibility Index Data on Cores

UT-02									
Core	Ligament Length (mm)	Notch Length (mm)	Peak Load (kN)	Time at P. Load (s)	Displ. at P. Load (s)	Test Rate (mm/min)	Fracture Energy (J/m^2)	Slope (kN/mm)	Strength (kPa)	FI
1	59.3	15.7	3.47	0.5704	0.423	50.116	657	-8.96	462.7	0.73
2	59.2	15.8	3.232	0.9424	0.725	50.066	886.6	-6.8	430.9	1.3
3	59.4	15.6	2.92	0.6696	0.502	50.057	706.9	-6.76	389.3	1.05
4	59.3	15.7	2.668	1.1904	1.002	50.006	1064.5	-3.71	355.7	2.87
UT-03										
Core	Ligament Length (mm)	Notch Length (mm)	Peak Load (kN)	Time at P. Load (s)	Displ. at P. Load (s)	Test Rate (mm/min)	Fracture Energy (J/m^2)	Slope (kN/mm))	Strength (kPa)	FI
1	59.4	15.6	1.8	0.9672	0.762	50.01	1152.4	-1.31	240	8.8
2	59.2	15.8	2.106	1.0912	0.875	50.016	1325.1	-1.36	280.8	9.77
3	59.5	15.5	2.364	1.0416	0.829	50.022	1321.6	-1.69	315.2	7.82
4	59.3	15.7	2.174	0.8928	0.692	50.02	1138.3	-1.65	289.9	6.9
UT-04										
Core	Ligament Length (mm)	Notch Length (mm)	Peak Load (kN)	Time at P. Load (s)	Displ. at P. Load (s)	Test Rate (mm/min)	Fracture Energy (J/m^2)	Slope (kN/mm)	Strength (kPa)	FI
1	59.3	15.7	2.624	1.0912	0.861	50.018	1425.3	-1.96	349.9	7.28
2	59.2	15.8	1.889	0.9424	0.739	50.03	886	-1.66	251.9	5.35
3	59.2	15.8	2.035	0.9176	0.723	50.023	1078	-1.38	271.3	7.84
4	59.5	15.5	2.343	1.1656	0.931	50.025	1246.4	-2.07	312.4	6.03
UT-05										
Core	Ligament Length (mm)	Notch Length (mm)	Peak Load (kN)	Time at P. Load (s)	Displ. at P. Load (s)	Test Rate (mm/min)	Fracture Energy (J/m^2)	Slope (kN/mm)	Strength (kPa)	FI
1	59.1	15.9	3.223	0.7936	0.604	50.042	1104.4	-3.97	429.5585	2.48
2	59.8	15.2	2.74	0.868	0.674	50.021	1337.1	-2.07	365.435	6.31
3	59.3	15.7	2.669	0.62	0.472	50.036	961.6	-2.54	351.645	3.5
4	59.4	15.6	2.573	0.6944	0.52	50.037	882.4	-3.22	343.371	2.55
UT-07										
Core	Ligament Length (mm)	Notch Length (mm)	Peak Load (kN)	Time at P. Load (s)	Displ. at P. Load (s)	Test Rate (mm/min)	Fracture Energy (J/m^2)	Slope (kN/mm)	Strength (kPa)	FI
1	59.2	15.8	3.386	0.9424	0.739	50.043	1587.7		451.5	
2	59.5	15.5	2.991	1.0664	0.832	50.025	1356.7	-2.93	398.8	4.63
3	59.3	15.7	3.246	0.8184	0.631	50.027	1349.9	-4.16	432.8	3.24
4	59.4	15.6	3.224	0.868	0.683	50.037	1312.8	-4.27	429.9	3.07

The thickness of all specimens was 50 mm

APPENDIX B: IDEAL CT Data on Cores

UT -02						
Core	Diameter (mm)	Layer Thickness (mm)	Fracture Energy (J/m^2)	Slope (kN/m)	Displacement at 75% (mm)	CT Index
1	150	50	7807.5	4.864	3.288	28.4
2	150	50	6989.4	5.54	3.096	21
3	150	50	9024.3	3.762	3.563	46
UT-03						
Core	Diameter (mm)	Layer Thickness (mm)	Fracture Energy (J/m^2)	Slope (kN/m)	Displacement at 75% (mm)	CT Index
1	150	50	8205.6	1.421	6.187	192.1
2	150	50	7231.9	1.759	4.408	97.4
3	150	50	8724.4	1.03	6.28	286
UT -04						
Core	Diameter (mm)	Layer Thickness (mm)	Fracture Energy (J/m^2)	Slope (kN/m)	Displacement at 75% (mm)	CT Index
1	150	50	8093.5	2.854	4.604	70.2
2	150	50	7292	2.927	4.365	58.5
3	150	50	6825.6	2.494	4.895	72
UT-05						
Core	Diameter (mm)	Layer Thickness (mm)	Fracture Energy (J/m^2)	Slope (kN/m)	Displacement at 75% (mm)	CT Index
1	150	50	9212.9	2.138	4.828	111.8
2	150	50	8719.5	1.919	4.42	108
3	150	50	7710.3	2.11	5.034	98.9
UT-07						
Core	Diameter (mm)	Layer Thickness (mm)	Fracture Energy (J/m^2)	Slope (kN/m)	Displacement at 75% (mm)	CT Index
1	150	50	12535	2.087	5.712	184.4
2	150	50	10632.5	2.984	4.662	89.3
3	150	50	10388.4	2.695	4.893	101.4

APPENDIX C: BBR Data on Cores

UT-02								
Specimen ID	W_{avg} (mm)	t_{avg} (mm)	-24°C		-18°C		-12°C	
			Stiffness at 60s (MPa)	*m*-value at 60s	Stiffness at 60s (MPa)	*m*-value at 60s	Stiffness at 60s (MPa)	*m*-value at 60s
A-UT-02-01	13.07	6.34	9.00E+03	0.117	6.67E+03	0.136	7.60E+03	0.148
A-UT-02-02	13.27	6.64	5.77E+03	0.137	5.81E+03	0.32		
A-UT-02-03	13.24	6.49	3.67E+03	0.033	1.22E+04	0.097	8.01E+03	0.131
A-UT-02-04	13.20	6.42	1.04E+04	0.109	1.24E+04	0.095	7.71E+03	0.102
A-UT-02-05	13.03	6.52	3.71E+03	0.026	1.02E+04	0.105	6.39E+03	0.234
A-UT-02-06	13.12	6.62	1.09E+04	0.083	9.19E+03	0.101	7.82E+03	0.141
A-UT-02-07	13.10	6.52	9.94E+03	0.104	8.59E+03	0.105	7.20E+03	0.117
A-UT-02-08	13.12	6.44	1.16E+04	0.094	1.22E+04	0.1	1.10E+04	0.116
A-UT-02-09	12.97	6.46	1.15E+04	0.09	9.18E+03	0.1	7.09E+03	0.134
A-UT-02-10	12.95	6.40	7.61E+03	0.084	1.39E+04	0.087	9.24E+03	0.126
Average	13.11	6.49	8410.00	0.088	10034.00	0.125	8006.67	0.139
Standard Deviation	0.11	0.09	3068.49	0.035	2638.18	0.070	1363.54	0.038
Coefficient of Variation	0.01	0.01	0.36	0.397	0.26	0.561	0.17	0.276
Standard Error	0.03	0.03	970.34	0.011	834.27	0.022	431.19	0.012
UT-03								
Specimen ID	W_{avg} (mm)	t_{avg} (mm)	-24°C		-18°C		-12°C	
			Stiffness at 60s (MPa)	*m*-value at 60s	Stiffness at 60s (MPa)	*m*-value at 60s	Stiffness at 60s (MPa)	*m*-value at 60s
A-UT-03-01	12.98	6.35	1.17E+04	0.143	9.93E+03	0.174	4.02E+03	0.225
A-UT-03-02	13.15	6.23	1.59E+04	0.128	1.05E+04	0.196	7.38E+03	0.23
A-UT-03-03	13.01	6.06	1.42E+04	0.128	1.15E+04	0.156	7.12E+03	0.217
A-UT-03-04	13.10	6.51	1.60E+04	0.133	1.04E+04	0.168	7.13E+03	0.222
A-UT-03-05	12.99	6.60	1.66E+04	0.148	1.04E+04	0.155	6.78E+03	0.246
A-UT-03-06	13.26	6.39	1.17E+04	0.157	1.13E+04	0.17	7.62E+03	0.221
A-UT-03-07	13.08	6.32	1.25E+04	0.128	1.02E+04	0.184	5.27E+03	0.237
A-UT-03-08	13.13	6.07	1.17E+04	0.15	8.52E+03	0.186	5.24E+03	0.255
A-UT-03-09	13.24	6.29	1.52E+04	0.116	1.04E+04	0.153	6.20E+03	0.191
A-UT-03-10	13.06	6.34	1.46E+04	0.134	1.17E+04	0.17	6.68E+03	0.211
Average	13.10	6.32	14010.00	0.137	10485.00	0.171	6344.00	0.226
Standard Deviation	0.10	0.17	1953.03	0.013	909.40	0.014	1155.59	0.018
Coefficient of Variation	0.01	0.03	0.14	0.092	0.09	0.084	0.18	0.080
Standard Error	0.03	0.05	617.60	0.004	287.58	0.005	365.43	0.006
UT-04								
Specimen ID	W_{avg} (mm)	t_{avg} (mm)	-24°C		-18°C		-12°C	
			Stiffness at 60s (MPa)	*m*-value at 60s	Stiffness at 60s (MPa)	*m*-value at 60s	Stiffness at 60s (MPa)	*m*-value at 60s
A-UT-04-01	12.99	6.42	1.43E+04	0.125	9.42E+03	0.134	6.37E+03	0.173
A-UT-04-02	13.23	6.37	1.91E+04	0.141	1.34E+04	0.174	8.63E+03	0.228
A-UT-04-03	13.01	6.52	1.71E+04	0.134	1.41E+04	0.173	8.72E+03	0.222
A-UT-04-04	13.54	6.24	1.67E+04	0.127	1.26E+04	0.16	7.86E+03	0.226
A-UT-04-05	13.37	6.33	1.88E+04	0.133	1.14E+04	0.173	6.59E+03	0.229
A-UT-04-06	13.01	6.32	1.43E+04	0.124	1.13E+04	0.156	7.91E+03	0.201
A-UT-04-07	13.15	6.50	2.02E+04	0.109	1.59E+04	0.164	9.72E+03	0.223
A-UT-04-08	13.32	6.45	1.39E+04	0.143	1.23E+04	0.174	5.73E+03	0.267
A-UT-04-09	13.36	6.35	1.56E+04	0.128	3.99E+03	0.091	6.39E+03	0.257
A-UT-04-10	13.19	6.34	1.50E+04	0.115	1.06E+04	0.201	5.98E+03	0.247
Average	13.22	6.38	16500.00	0.128	11501.00	0.160	7390.00	0.227
Standard Deviation	0.18	0.09	2251.91	0.011	3217.43	0.030	1360.18	0.027
Coefficient of Variation	0.01	0.01	0.14	0.083	0.28	0.185	0.18	0.119
Standard Error	0.06	0.03	712.12	0.003	1017.44	0.009	430.13	0.009

UT-05								
Specimen ID	W_{avg} (mm)	t_{avg} (mm)	-24°C		-18°C		-12°C	
			Stiffness at 60s (MPa)	*m*-value at 60s	Stiffness at 60s (MPa)	*m*-value at 60s	Stiffness at 60s (MPa)	*m*-value at 60s
A-UT-05-01	13.21	6.24	1.72E+04	0.084	9.19E+03	0.132	9.93E+03	0.165
A-UT-05-02	13.18	6.31	6.98E+03	0.048	1.61E+04	0.141	9.73E+03	0.177
A-UT-05-03	12.92	6.11	1.66E+04	0.095	1.25E+04	0.131	7.87E+03	0.173
A-UT-05-04	13.05	6.51	3.53E+03	0.037	1.21E+04	0.111	9.82E+03	0.19
A-UT-05-05	13.19	6.22	1.58E+04	0.105	1.28E+04	0.141	5.42E+03	0.17
A-UT-05-06	13.23	6.29	1.06E+04	0.109	1.11E+04	0.134	7.28E+03	0.167
A-UT-05-07	13.21	6.43	2.21E+04	0.116	1.52E+04	0.141	1.20E+04	0.22
A-UT-05-08	13.28	6.19	1.77E+04	0.121	1.59E+04	0.143	1.07E+04	0.189
A-UT-05-09	13.05	6.36	1.68E+04	0.103	1.04E+04	0.128	8.91E+03	0.181
A-UT-05-10	13.25	6.21	1.61E+04	0.111	1.36E+04	0.136	1.09E+04	0.166
Average	13.16	6.29	14341.00	0.093	12889.00	0.134	9256.00	0.180
Standard Deviation	0.11	0.12	5588.56	0.029	2335.31	0.009	1942.93	0.017
Coefficient of Variation	0.01	0.02	0.39	0.308	0.18	0.071	0.21	0.093
Standard Error	0.04	0.04	1767.26	0.009	738.49	0.003	614.41	0.005
UT-07								
Specimen ID	W_{avg} (mm)	t_{avg} (mm)	-24°C		-18°C		-12°C	
			Stiffness at 60s (MPa)	*m*-value at 60s	Stiffness at 60s (MPa)	*m*-value at 60s	Stiffness at 60s (MPa)	*m*-value at 60s
A-UT-07-01	13.04	6.43	1.95E+04	0.141	1.33E+04	0.165	9.83E+03	0.217
A-UT-07-02	12.97	6.42	1.68E+04	0.12	1.35E+04	0.135	8.65E+03	0.249
A-UT-07-03	12.58	6.44	1.47E+04	0.102	1.31E+04	0.161	8.10E+03	0.196
A-UT-07-04	12.94	6.33	1.04E+04	0.098	8.66E+03	0.154	7.23E+03	0.208
A-UT-07-05	12.94	6.54	8.10E+03	0.142	1.19E+04	0.159	7.81E+03	0.203
A-UT-07-06	12.39	6.36	1.74E+04	0.122	9.39E+03	0.155	7.94E+03	0.205
A-UT-07-07	13.04	6.38	1.51E+04	0.111	1.37E+04	0.149	7.71E+03	0.187
A-UT-07-08	13.17	6.29	1.37E+04	0.098	9.86E+03	0.145	6.68E+03	0.163
A-UT-07-09	12.36	6.60	1.67E+04	0.109	1.20E+04	0.143	8.41E+03	0.211
A-UT-07-10	13.01	6.55	1.75E+04	0.118	1.11E+04	0.185	6.96E+03	0.202
Average	12.84	6.43	14990.00	0.116	11651.00	0.155	7932.00	0.204
Standard Deviation	0.29	0.10	3479.29	0.016	1831.49	0.014	909.45	0.022
Coefficient of Variation	0.02	0.02	0.23	0.137	0.16	0.089	0.11	0.107
Standard Error	0.09	0.03	1100.25	0.005	579.17	0.004	287.59	0.007